



Available online at [www.sciencedirect.com](http://www.sciencedirect.com)

ScienceDirect



Journal of the Franklin Institute 360 (2023) 7501–7534

[www.elsevier.com/locate/jfranklin](http://www.elsevier.com/locate/jfranklin)

# Distributed secure consensus control of nonlinear multi-agent systems under sensor and actuator attacks

Sergey Gorbachev<sup>a</sup>, Yang Yang<sup>b,\*</sup>, Qidong Liu<sup>b</sup>, Jingzhi Ge<sup>b</sup>,  
Dong Yue<sup>b</sup>, Ashish Mani<sup>a</sup>, Dmytro Shevchuk<sup>a</sup>

<sup>a</sup>*School of Artificial Intelligence, Chongqing University of Education, Chongqing 400065, China*

<sup>b</sup>*College of Automation & College of Artificial Intelligence, Nanjing University of Posts and Telecommunications, Nanjing 210023, China*

Received 12 January 2022; received in revised form 1 April 2023; accepted 21 May 2023

Available online 31 May 2023

---

## Abstract

In this paper, we focus on an output secure consensus control issue for nonlinear multi-agent systems (MASs) under sensor and actuator attacks. Followers in an MAS are in strict-feedback form with unknown control directions and unknown dead-zone input, where both sensors and nonlinear characteristics of dead-zone in actuators are paralyzed by malicious attacks. To deal with sensor attacks, uncertain dynamics in individual follower are separated by a separation theorem, and estimation parameters are introduced for compensating and mitigating the influence from adversaries. The influence from actuator attacks are treated as a total displacement in a dead-zone nonlinearity, and an upper bound, as well as its estimation, is introduced for this displacement. The dead-zone nonlinearity, sensor attacks and unknown control gains are gathered together regarded as composite unknown control directions, and Nussbaum functions are utilized to address the issue of unknown control directions. A distributed secure consensus control strategy is thus developed recursively for each follower in the framework of surface control method. Theoretically, the stability of the closed-loop MAS is analyzed, and it is proved that the MAS achieves output consensus in spite of nonlinear dynamics and malicious attacks. Finally, theoretical results are verified via a numerical example and a group of electromechanical systems.

© 2023 The Franklin Institute. Published by Elsevier Inc. All rights reserved.

---

\* Corresponding author.

E-mail addresses: [gorbachev@cque.edu.cn](mailto:gorbachev@cque.edu.cn) (S. Gorbachev), [yyang@njupt.edu.cn](mailto:yyang@njupt.edu.cn) (Y. Yang).

## 1. Introduction

Multi-agent systems (MASs) have been widely applied in a variety of disciplines [1,2], such as transportation systems [3], electro-mechanical systems [4], on account of their flexibility and scalability, and distributed consensus of MASs has been concerned by control community. Owing to communication over networks, information in an MAS is vulnerable to malicious attacks. There exist cyber threats in an MAS, and these attacks degrade cooperative performance even result in instability of an networked system. It is a critical topic to develop distributed secure consensus control of MASs.

Distributed control of MASs has achieved fruitful results [5–7]. Authors proposed a novel non-singular terminal sliding-mode distributed controller in [8] to achieve fixed-time consensus of an MAS, and the proposed sliding-mode controller was able to avoid singularities and achieve accurate convergence. For a nonlinear MAS, Hong studied a robust consensus problem under a weighted undirected topology and proposed a distributed fixed-time nonlinear control protocol [9]. A distributed adaptive fault-tolerant consensus of a class of uncertain nonlinear second-order MASs was reported in [10]. By designing adaptive schemes and state feedback control gains, a novel distributed control strategy was constructed to ensure the asymptotic consensus of agents in the presence of actuator failure, uncertainty and nonlinear dynamics. Few of the above results [6–10] considered influence from cyber attacks.

Secure control of MASs under cyber attacks, such as sensor or actuator attacks, has been studied [11,12]. For self-generated false data injection (FDI) attacks that are independent of real-time data of CPSs, a necessary and sufficient condition of attack parameters is proposed in [13], and generated FDI attacks achieve complete stealthiness. Considering a CPS with sensor and actuator attacks, Gao et al. designed a state controller based on estimation information to cope with attacks, and they further designed a self-triggering controller by dissipativity approach for saving resources [14]. In [15], authors mitigated adversarial attacks over a networked physical system by estimating of unknown attacks directly. A secure control problem for T-S fuzzy systems subjected to stealthy sensor and actuator attacks simultaneously is studied in [16] with a Luenberger-observer-based anomaly detector. Observer-based finite-time  $H_\infty$  control problem for interconnected fuzzy systems with quantization and random network attacks is investigated in [17], where two types of network attacks including denial of service (DoS) and FDI attacks are considered. A secure state estimation and control problem of CPSs with sensors and actuators both under the threat of intermittent FDI attacks is studied in [18], and with the help of a specific filter gain, both sensor attacks and actuator attack can be detected. A stabilization problem of a distributed networked control system under the effect of a stochastic deception attack at the sensor-controller end is examined in [19], and a hybrid aperiodic triggering mechanism is employed to against cyber-attacks. For security control research of linear multi-agent systems, authors design a distributed adaptive compensator and integrate it with a distributed control protocol in [20]. Most results on sensor and actuator attacks [14–20] were for linear MASs.

Since dead-zone input and unknown control directions are common in practical nonlinear systems, the two topics have been extensively studied. Unknown dead-zone input was reported [21–26] for output tracking problem. By using online estimation technique, an adaptive variable was designed to estimate infimum of unknown dead-zone parameters [24]. For an optimal control problem of a nonlinear system with nonaffine dead-zone input, gradient rules were employed to calculate adaptive laws for the dead-zone parameters [25]. With the help of equivalence dead-zone inverse, a nonlinear system with unknown dead-zone input was

converted to a system without the dead-zone [26]. Another issue in nonlinear systems was that control directions may not be available [27–32]. A Nussbaum gain function was introduced in controller design with unknown control directions. This method was proposed by Nussbaum [27], and it effectively approximated the sign of control directions. Using Nussbaum gain functions and dynamic signals, a fuzzy adaptive fault-tolerant control problem was developed based on approximation [30]. For a non-strict feedback structure, Yu et al., combined parameterization of neural networks (NNs), variable separation technique with Nussbaum gain function method [31]. Based on a Nussbaum type function, authors in [32] studied nonlinear MASs with unknown control directions in a stochastic topology.

Although many efforts have been taken on consensus control of MASs [11–32], there still exist technical gaps for MASs in the presence of malicious attacks. The existing researches about sensor and actuator attacks mainly focus on linear MAS [14–20] but few report on nonlinear MASs. Followers in an MAS hold state-related nonlinear dynamics, and their state information and control signals may be paralyzed due to sensor and actuator attacks. Accordingly, the characteristics of nonlinear dynamics will be more or less affected by these attacks, and system performance will be degraded by conventional control methods. Although there are some security control results of MAS under sensor attacks, these methods only consider that the follower's own sensor is attacked [16]. In the actual communication, neighbors' information measured by sensors may be attacked by adversaries when it is transmitted to a network, which will degrade the tracking consensus performance. Furthermore, if the follower with dead-zone input is under actuator attacks, nonlinear characteristics of a dead zone will be modified. The displacement of dead-zone characteristics will affect existing dead zone control methods to stabilize the system [22]. How to deal with the displacement of dead-zone characteristics after actuator attacks is one of the motivations of this paper.

To fill in these technical gaps, we consider nonlinear MASs in the presence of sensor and actuator attacks and unknown control directions and develop secure strategy with compensation items for alleviating attacking impacts. Combining Nussbaum function, continuous function separation theorem and adaptive compensation technology, we address the problem of FDI attack on actuators with dead zone and unknown control direction. Furthermore, the continuous function separation theorem and adaptive compensation mechanism are used to deal with the situation that neighbor information is under sensors attacks in tracking consensus problem. The main contributions of this paper are summarized as follows.

(1) We take secure control of a nonlinear MAS with dead-zone inputs and unknown control directions against malicious attacks into account, and this MAS is suffered from both actuator and sensor attacks. Different from secure control problem for linear MASs [14–20], the topic in this paper is for nonlinear MASs. Under sensor attacks, it is more difficult to deal with unknown state-dependent nonlinear dynamics due to unavailable real states. Compared with the nonlinear MAS under actuator and sensor attacks in [33], we further consider a situation that, in a nonlinear MAS, each follower has a dead-zone input and unknown control directions. These are more practical for industrial applications.

(2) A function separation theorem with a scaling of inequality is introduced in our strategy to deal with sensor attacks on information from followers themselves and neighbors. Compared with the method in [33] who only depends on local information from individual follower, our strategy further includes paralyzed information from neighbors. By introducing the function separation theorem, uncertain dynamics in a follower and its neighbors influenced by adversaries are separated, and adaptive parameters are developed to compensate for the influence.

(3) Nussbaum functions and adaptive compensation technology are combined in our strategy for each follower with dead-zone input and unknown control directions in the presence of actuator attacks. Due to displacement in the nonlinearity of dead zone on account of actuator attacks, we reconstruct a dead-zone model in this scenario, and, by the mean value theorem, we divide the rake ratio and displacement separately. The rake ratio in a dead zone with an unknown control gain and sensor attack information are gathered together and treated as a new unknown control direction. Nussbaum functions are then employed to estimate this new direction. An adaptive compensation technique is introduced to eliminate the influence from displacement.

**Outline:** The remaining part of this paper is organized as follows. Section II presents necessary preliminaries and problem formulation. In Section III, we propose a distributed secure consensus control strategy as well as stability analysis. Two simulations with comparison results are illustrated in Section IV, and the conclusions are drawn in Section V.

**Notation:**  $\mathbb{R}^n$  denotes the  $n$ -dimensional Euclidean space.  $1_N$  is a  $N \times 1$  column vector with all elements being 1.  $\|\cdot\|$  stands for the Euclidean norm of a vector.  $\otimes$  represents the Kronecker product.  $\text{rank}(\cdot)$  denotes the rank of a matrix.

## 2. Problem description and preliminaries

### 2.1. System description

Consider a nonlinear MAS consisting of  $N$  followers and one leader. The dynamics of  $i$ th follower are in the following strict-feedback form

$$\begin{cases} \dot{x}_{i,m} = f_{i,m}(\bar{x}_{i,m}) + g_{i,m}(\bar{x}_{i,m})x_{i,m+1}, & i = 1, \dots, N, m = 1, \dots, n_i - 1 \\ \dot{x}_{i,n_i} = f_{i,n_i}(\bar{x}_{i,n_i}) + g_{i,n_i}(\bar{x}_{i,n_i})u_i, \\ y_i = x_{i,1}, \end{cases} \quad (1)$$

where  $\bar{x}_{i,k} = [x_{i,1}, \dots, x_{i,k}]^T \in \mathbb{R}^k$ ,  $k = 1, \dots, n_i$  is the state vector,  $y_i \in \mathbb{R}$  is the output of  $i$ th follower,  $f_{i,k}(\bar{x}_{i,k})$  is an unknown smooth nonlinear function,  $g_{i,k}$  is a non-zero unknown smooth gain function and  $u_i \in \mathbb{R}$  is control input with dead-zone, satisfying

$$u_i = D_i(v_i) = \begin{cases} H_{ir}(v_i), & v_i \geq p_{ir} \\ 0, & -p_{il} < v_i < p_{ir} \\ H_{il}(v_i), & v_i \leq -p_{il} \end{cases} \quad (2)$$

with  $v_i$  representing the input of the dead-zone and  $p_{ir}$  and  $p_{il}$  being uncertain bounded breakpoints of the dead-zone.

**Remark 1.** An input dead zone means that a control input is not feasible within a certain range. In practical engineering, there often exists a dead zone in an actuator for most engineering systems, such as backlash of gears, valves, DC servo motors, continuous stirred tank reactors [34], and many other electro-mechanical systems [35].

**Assumption 1.** For the unknown gain  $g_{i,k}$ , there exists an upper bound  $\bar{g} > 0$  such that  $0 < |g_{i,k}| < \bar{g}$ ,  $k = 1, \dots, n_i$ .

**Assumption 2.** The nonlinearities  $H_{ir}(v_i)$  and  $H_{il}(v_i)$  in a dead-zone are differentiable. There exist positive constants  $H_{ir0}$ ,  $H_{ir1}$ ,  $H_{il0}$  and  $H_{il1}$  such that

$$0 < H_{ir0} \leq H'_{ir}(v_i) \leq H_{ir1}, \quad \text{if } v_i(t) \geq p_{ir}$$

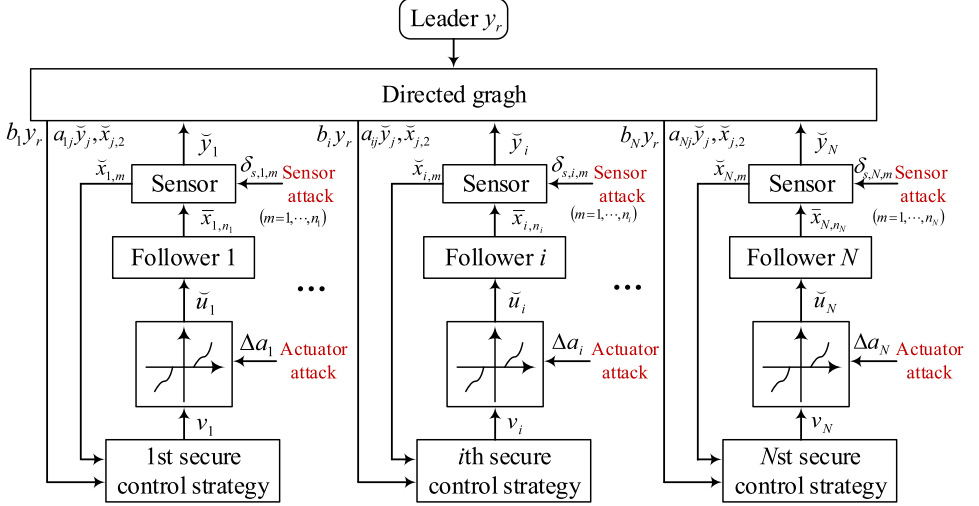


Fig. 1. An MAS subjected to cyber attacks.

$$0 < H_{il0} \leq H_{il}'(v_i) \leq H_{il1}, \quad \text{if } v_i(t) < -p_{il}$$

where  $H_{ir}'(v_i) = dH_{ir}(s)/ds|_{s=v_i}$ , and  $H_{il}'(v_i) = dH_{il}(s)/ds|_{s=v_i}$ .

Denote  $H_{i,\min} = \min\{H_{ir0}, H_{il0}\}$  and  $H_{i,\max} = \max\{H_{ir1}, H_{il1}\}$ . According to [Assumption 1](#) and the mean value theorem, there exists a constant  $\xi_{ir} \in (p_{ir}, v_i)$  when  $v_i(t) \geq p_{ir}$ , a constant  $\xi_{il} \in (v_i, -p_{il})$  when  $v_i(t) < -p_{il}$ , such that the control input with dead-zone (2) can be expressed as

$$u_i = D_i(v_i) = \bar{H}_i v_i + d_i(v_i), \quad (3)$$

where  $\bar{H}_i = \begin{cases} H_{ir}'(\xi_{ir}), & v_i \geq p_{ir} \\ H_{i0}', & -p_{il} < v_i < -p_{ir} \\ H_{il}'(\xi_{il}), & v_i \leq -p_{il} \end{cases}$  is the rake ratio of the dead-zone,  $d_i(v_i) = \begin{cases} -H_{ir}'(\xi_{ir})p_{ir}, & v_i \geq p_{ir} \\ -H_{i0}'v_i, & -p_{il} < v_i(t) < p_{ir} \\ -H_{il}'(\xi_{il})p_{il}, & v_i(t) \leq -p_{il} \end{cases}$  and  $H_{i0}'$  satisfies  $H_{i,\min} \leq H_{i0}' \leq H_{i,\max}$ .

## 2.2. Cyber attack model

In this paper, we assume that each follower in an MAS is subject to cyber attacks, including sensor and actuator attacks. Its the structure is shown in [Fig. 1](#).

### 2.2.1. Sensor attack model

In the cyber transmission of the information for feedback control, unexpected data may be injected into sensors. Measured state information is stealthily monitored by adversarial attackers and deception attack signals are maliciously injected into measured states [15]. For example, when measurement of voltage data of a power plant is under sensors attacks, measured voltage may deviate from the true value, and then the key equipment will fail and

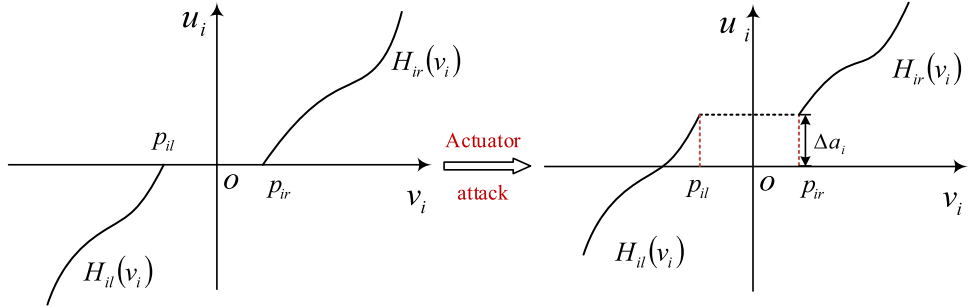


Fig. 2. An illustrative diagram of an actuator attack.

the system works in an unstable manner [36]. In this case, deception attack signals may depend on state variables. We denote the sensor attack is  $\delta_{s,i,m}$ ,  $i = 1, \dots, N$ ,  $m = 1, \dots, n_i$ , and the paralyzed state of each follower is

$$\ddot{x}_{i,m} = \delta_{s,i,m} + x_{i,m}, \quad (4)$$

where  $\delta_{s,i,m} = \omega_{i,m}x_{i,m}$ , and  $\omega_{i,m}$  is unknown attack time-varying weight. Define  $\lambda_{i,m} = 1 + \omega_{i,m}$ , then  $\ddot{x}_{i,m} = \lambda_{i,m}x_{i,m}$ ,  $x_{i,m} = \lambda_{i,m}^{-1}\ddot{x}_{i,m}$ .

**Assumption 3** [33]. There exists a positive unknown constants  $\lambda_{i,m}^*$  such that  $|\lambda_{i,m}| \leq \bar{\lambda}_{i,m} = C \exp(\lambda_{i,m}^* t)$ , where  $C > 0$ .

**Remark 2.** For bounded  $\lambda_{i,m}$ , we take a bounded sensor attack into account in this paper. For  $|\lambda_{i,m}| \leq C \exp(\lambda_{i,m}^* t)$  in Assumption 3,  $\dot{\omega}_{i,m} \leq C\lambda_{i,m}^* \exp(\lambda_{i,m}^* t)$  is obtained by deriving  $\lambda_{i,m}$ . Further, we get  $|\frac{\dot{\omega}_i}{1+\omega_i}| < \lambda_{i,m}^*$ , and according to the sensor attack model, we have  $|\dot{\lambda}_{i,m}\lambda_{i,m}^{-1}| \leq \lambda_{i,m}^*$ .

### 2.2.2. Actuator attack model

Actuator attacks often act on an actuator, and they tamper amplitudes of control signals stealthily. This action degrades system performance and even leads to instability [15]. For example, acceleration and steering actuators of autonomous vehicles/aircraft may be attacked by actuators, which make the vehicles/aircraft deviate from a desired trajectory by injecting false information [37]. Therefore, actuator attacks are considered to be superimposed on control signals in this paper, and it modifies the nonlinear characteristic of the dead zone. We denote the displacement as  $\Delta a_i$ , where  $\Delta a_i$  is a unknown constant, and the control input becomes

$$\ddot{u}_i = \check{D}_i(v_i) = \begin{cases} H_{ir}(v_i) + \Delta a_i, & v_i \geq p_{ir}, \\ 0 + \Delta a_i, & -p_{il} < v_i < p_{ir}, \\ H_{il}(v_i) + \Delta a_i, & v_i \leq -p_{il}. \end{cases} \quad (5)$$

An illustrative diagram of this attack is shown in Fig. 2.

According to Assumption 2 and (3), the control input with an actuator attack yields

$$\ddot{u}_i = \check{D}_i(v_i) = \bar{H}_i v_i + \check{d}_i(v_i(t)), \quad (6)$$

where  $\check{d}_i(v_i(t)) = \begin{cases} -H'_{ir}(\xi_{ir})p_{ir} + \Delta a_i, & v_i \geq p_{ir} \\ -H'_{il}v_i + \Delta a_i, & -p_{il} < v_i(t) < p_{ir} \\ -H'_{il}(\xi_{il})p_{il} + \Delta a_i, & v_i(t) \leq -p_{il} \end{cases}$ . Accordingly, from (4) and (6), the dynamics of  $i$ th follower (1) with sensor and actuator attacks are

$$\begin{cases} \dot{x}_{i,m} = f_{i,m}(\bar{x}_{i,m}) + g_{i,m}x_{i,m+1}, & i = 1, \dots, N, \quad m = 1, \dots, n_i - 1, \\ \dot{x}_{i,n_i} = f_{i,n_i}(\bar{x}_{i,n_i}) + g_{i,n_i}\check{u}_i, \\ \dot{\check{x}}_{i,m} = \lambda_{i,m}x_{i,m}, \\ \check{y}_i = \check{x}_{i,1}, \end{cases} \quad (7)$$

where attacks render the output of each follower from  $y_i = x_{i,1}$  to  $\check{y}_i = \check{x}_{i,1}$  correspondingly.

**Remark 3.** In cyber transmission of information for feedback control, unexpected data may be injected into sensors or actuators. Measured state information is stealthily monitored by adversarial attackers and deception attack signals are maliciously injected into measured states. Accordingly, deception attack signals may depend on state variables. Thus, the sensor attack  $\delta_{s,i,m}$  is parameterized as  $\delta_{s,i,m} = \omega_{i,m}x_{i,m}$  in this paper. Also, there exist actuator attacks in the real world, and they tamper amplitudes of control signals stealthily. This attack  $\Delta a_i$  superimposed on the control signal will paralyze the actuator with dead zone in this paper. Energy of adversaries is constraint and it is a reasonable assumption that attack signals are bounded. Attacks are often maliciously and stealthily launched to undermine the authenticity of sensor measurement data or actuator data.

**Remark 4.** Indeed, there often exist failures from physical devices and attacks from network communication simultaneously in an MAS [43]. Intuitively, the model of actuator faults is usually described as  $u_i = \zeta_i v_i + u_{i,0}$ , where  $\zeta_i \in (0, 1)$  denotes the unknown actuator/sensor effectiveness,  $v_i$  is the actuator input signal, and  $u_{i,0}$  is an unknown bounded time-varying function representing bias faults. Also, the model of sensor faults is as  $\check{x}_i = \xi_i x_i + x_{i,0}$ , where  $\xi_i \in (0, 1)$  denotes the unknown sensor effectiveness, and  $x_{i,0}$  is an unknown bounded time-varying function representing information drift in a sensor. Although the form of failures and attacks is similar in mathematical expression, there are two main differences. (1) The failure coefficient  $\zeta_i$  and  $\xi_i$  are generally in  $(0, 1)$ , but there is no such limit in the unknown bounded attack weight. (2) They occur in different layers, where faults are in the physical layer, and attacks often occur in the cyber layer. We only aim at a control strategy for possible attacks from actuators and sensors. It is worth mentioning that the concepts of attacks and failures are not the same, and we assume that attack detection provides real-time signals. More related research can be found in [13,38].

### 2.3. Graph theory

Consider an MAS consisting of  $N$  followers, and the information communication between followers is denoted by a directed graph  $\wp(\mathcal{V}, \mathcal{E}, \mathcal{A})$ , where  $\mathcal{V} = \{v_1, \dots, v_N\}$  is a set of followers  $v_i (i = 1, \dots, N)$ ,  $\mathcal{E} \subseteq \mathcal{V} \times \mathcal{V}$  is an edge set, and  $\mathcal{A} = [a_{ij}]_{N \times N}$  represents an adjacency matrix with  $a_{ij} = \begin{cases} 1, & (v_j, v_i) \in \mathcal{E}, \\ 0, & (v_j, v_i) \notin \mathcal{E}. \end{cases}$  indicates that the Follower  $v_i$  can directly obtain the information of Follower  $v_j$ . A set of the neighbors of the  $i$ th follower is defined as  $\Pi_i = \{j | (v_j, v_i) \in \mathcal{E}\}$ . The Laplacian matrix of a directed graph  $\wp$  is defined as

$$\mathcal{L} = [l_{ij}]_{N \times N}, \text{ where } l_{ij} = \begin{cases} -a_{ij}, & i \neq j \\ \sum_{j=1, i \neq j}^N a_{ij}, & i = j \end{cases}.$$

The communication between  $N$  followers and one leader can be represented by an augmented graph  $\wp_0(\mathcal{V}_0, \mathcal{E}_0, \mathcal{A}_0)$ , where  $\mathcal{V}_0 = \{v_0, v_1, \dots, v_N\}$  is a set of  $N$  followers and leader  $v_0$ . With the augmented graph  $\wp_0$ , the Laplacian matrix is  $\mathcal{L}_0 = \begin{bmatrix} 0 & 0_{1 \times N} \\ -b & \mathcal{L} + \mathcal{B} \end{bmatrix}_{(N+1) \times (N+1)}$ , where  $\mathcal{B} = \text{diag}\{b_1, \dots, b_N\}$ ,  $b = [b_1, \dots, b_N]^T$ . If Follower  $v_i$  can obtain information from the leader, we have  $b_i = 1$ , otherwise  $b_i = 0$ . Moreover, if there exists at least one root node that has directed paths to all other agents in a graph, it is said that the directed graph has a directed spanning tree.

**Assumption 4.** The directed graph  $\wp_0$  contains a spanning tree and the leader is the root node.

**Assumption 5.** The state information  $x_{j,2}$  of the  $j$ th follower is available for the  $i$ th follower,  $j \in \Pi_i$ ,  $i = 1, \dots, N$ ,  $j = 1, \dots, N$ , and  $i \neq j$ .

#### 2.4. Other assumptions and lemmas

The following assumptions and lemmas, related to Nussbaum functions and useful inequalities, are also introduced.

**Lemma 1** [31,32]. *Consider a Nussbaum function  $N_{i,j}(\kappa_{i,j})$ , if there exists a positive definite, radially unbounded function  $V(t)$  such that the following inequality holds*

$$V(t) \leq \sum_{i=1}^N \int_0^t (g_{i,j}(\cdot)N_{i,j}(\kappa_{i,j}) + 1)\dot{\kappa}_{i,j}(s)ds + d, \quad (8)$$

$V(t)$ ,  $\kappa_{i,j}$  and  $\sum_{i=1}^N \int_0^t g_{i,j}(\cdot)N_{i,j}(\kappa_{i,j})\dot{\kappa}_{i,j}(s)ds$  are all bounded, where  $g_{i,j}(\cdot)$  is an unknown function, and  $d$  is a positive constant for  $t \in [0, \infty)$ .

**Assumption 6.** The leader signal  $y_r \in \mathbb{R}$  and its derivative  $\dot{y}_r \in \mathbb{R}$  and second derivative  $\ddot{y}_r \in \mathbb{R}$  are bounded and available for the  $i$ th follower satisfying  $b_i = 1$ ,  $i = 1, \dots, N$ .

**Lemma 2** [44]. *For a continuous function  $f(x, y) \in \mathbb{R}$ , where  $x \in \mathbb{R}^m$ ,  $y \in \mathbb{R}^n$ , there exist two smooth functions,  $c(x)$  and  $d(y)$ , such that the inequality  $|f(x, y)| \leq c(x)d(y)$  holds.*

**Lemma 3.** *The following inequality  $0 \leq |z| - z \cdot sg(z) \leq \sigma$  holds, where  $z \in \mathbb{R}$ ,  $\sigma = \exp(-at) > 0$ ,  $a$  is a positive constant, and  $sg(z) = \frac{z}{\sqrt{z^2 + \sigma^2}}$ .*

#### 2.5. Control objective

**The objective of this paper** is to design a distributed consensus secure control strategy for a nonlinear MAS with followers in Eq. (1) such that the output  $y_i$  of each follower achieves consensus with the trajectory  $y_r$  of the leader in spite of sensor and actuator attacks, i.e.,  $\lim_{t \rightarrow \infty} \|S\| \leq \sigma$ , where  $S = [S_1, \dots, S_N]^T$ ,  $S_i = y_i - y_r$  is the consensus error,  $i = 1, \dots, N$ , and  $\sigma$  is a bounded positive constant, and all closed-loop signals in the MAS are bounded.

**Remark 5.** Indeed, random attacks are common in the real word. Actuator and sensor attacks in this paper are not available to followers, and this means that sensors and actuators occur aperiodically. That is to say, exact instants of attacks in this paper are unknown, which is similar to random attacks in this respect. In fact, our secure control strategy deals with unknown attacks with error signals according to the compensation principle. From this perspective, we pay more attention on amplitude alleviation for attacks.

### 3. Distributed secure consensus control design

In this part, a distributed consensus secure control strategy is developed by combining the dynamic surface control (DSC) method [39,40] and the function separation theorem.

Define the output error  $e_{i,1}$ , surface error  $e_{i,m}$  and the filter error  $\varpi_{i,m}$  as

$$\begin{cases} e_{i,1} = \sum_{j=1}^N a_{ij}(\check{y}_i - \check{y}_j) + b_i(\check{y}_i - y_r), \\ e_{i,m} = \check{x}_{i,m} - z_{i,m}, \end{cases} \quad (9)$$

and

$$\varpi_{i,m} = z_{i,m} - \alpha_{i,m}, \quad (10)$$

where  $z_{i,m}$  and  $\alpha_{i,m}$  are the output of a first-order filter and a virtual control law, respectively,  $m = 2, \dots, n_i$ , and they will be designed later. The secure control strategy in each follower is composed of  $n_i$  steps.

**Step 1:** From Eq. (9), we take time derivative of  $e_{i,1}$  along with Eq. (7) yielding

$$\dot{e}_{i,1} = \sum_{j=1}^N a_{ij}(\dot{\lambda}_{i,1}x_{i,1} + \lambda_{i,1}\dot{x}_{i,1}) + b_i(\dot{\lambda}_{i,1}x_{i,1} + \lambda_{i,1}\dot{x}_{i,1}) - \sum_{j=1}^N a_{ij}\dot{\check{x}}_{j,1} - b_i\dot{y}_r. \quad (11)$$

From (11), we obtain

$$\begin{aligned} e_{i,1}\dot{e}_{i,1} &= (d_i + b_i)(e_{i,1}\dot{\lambda}_{i,1}\lambda_{i,1}^{-1}\check{x}_{i,1} + g_{i,1}(x_{i,1})e_{i,1}\check{x}_{i,2} + \lambda_{i,1}f_{i,1}(x_{i,1})e_{i,1}) \\ &\quad - \sum_{j=1}^N a_{ij}(e_{i,1}\dot{\lambda}_{j,1}\lambda_{j,1}^{-1}\check{x}_{j,1} + g_{j,1}(x_{j,1})e_{i,1}\check{x}_{j,2} + \lambda_{j,1}f_{j,1}(x_{j,1})e_{i,1}) - b_i e_{i,1}\dot{y}_r. \end{aligned} \quad (12)$$

For Eq. (12), applying Lemma 3 and Assumption 3, one has

$$e_{i,1}\dot{\lambda}_{i,1}\lambda_{i,1}^{-1}\check{x}_{i,1} \leq \lambda_{i,1}^*(\sigma_{i,1} + \frac{(e_{i,1}\check{x}_{i,1})^2}{\sqrt{(e_{i,1}\check{x}_{i,1})^2 + \sigma_{i,1}^2}}) \quad (13)$$

and

$$e_{i,1}\dot{\lambda}_{j,1}\lambda_{j,1}^{-1}\check{x}_{j,1} \leq \underline{\lambda}_{i,1}^*(\sigma_{i,1} + \frac{(e_{i,1}\check{x}_{j,1})^2}{\sqrt{(e_{i,1}\check{x}_{j,1})^2 + \sigma_{i,1}^2}}), \quad (14)$$

where  $\sigma_{i,1} = \exp(-a_{i,1}t)$ , and  $a_{i,1}$  is a positive constant.

Due to the influence of sensor attacks in Eq. (4), the actual state of follower is not available. It needs to separate the attacked state by Lemma 2. Substituting  $x_{i,1} = \lambda_{i,1}^{-1}\check{x}_{i,1}$  into  $\lambda_{i,1}f_{i,1}(x_{i,1})$ , then  $|f_{i,1}(x_{i,1})| = |f_{i,1}(\lambda_{i,1}^{-1}\check{x}_{i,1})|$ . There exist an unknown positive constant  $\bar{w}_{i,1}$  satisfying  $w_{i,1}(\lambda_{i,1}^{-1}) \leq \bar{w}_{i,1}$  and a known smooth function  $\Psi_{i,1}(\check{x}_{i,1})$  such that

$$\begin{aligned} |f_{i,1}(x_{i,1})| &= |f_{i,1}(\lambda_{i,1}^{-1}\check{x}_{i,1})| \\ &\leq w_{i,1}(\lambda_{i,1}^{-1})\Psi_{i,1}(\check{x}_{i,1}) \\ &\leq \bar{w}_{i,1}\Psi_{i,1}(\check{x}_{i,1}). \end{aligned} \quad (15)$$

Denote  $\Theta_{i,1}^* = \bar{w}_{i,1}\bar{\lambda}_{i,1}$  and  $\underline{\Theta}_{i,1}^* = \bar{w}_{j,1}\bar{\lambda}_{j,1}$ . By Lemma 3, Assumption 3 and Eq. (15), one has

$$e_{i,1}\lambda_{i,1}f_{i,1}(x_{i,1}) \leq \Theta_{i,1}^* \left( \sigma_{i,1} + \frac{(e_{i,1}\Psi_{i,1})^2}{\sqrt{(e_{i,1}\Psi_{i,1})^2 + \sigma_{i,1}^2}} \right) \quad (16)$$

and

$$e_{i,1}\lambda_{j,1}f_{j,1}(x_{j,1}) \leq \underline{\Theta}_{i,1}^* \left( \sigma_{i,1} + \frac{(e_{i,1}\Psi_{j,1})^2}{\sqrt{(e_{i,1}\Psi_{j,1})^2 + \sigma_{i,1}^2}} \right). \quad (17)$$

**Remark 6.** Compared with a single system that only its own states under sensor attacks [33], an MAS suffered from sensor attacks is considered in this paper, where information from neighbors may also be paralyzed by attack signals for each follower. In this sense, we are going to design adaptive parameters for  $\underline{\lambda}_{i,1}^*$  and  $\underline{\Theta}_{i,1}^*$  to compensate paralyzed information from neighbors in the secure control strategy.

For the  $\sum_{j=1}^N a_{ij}g_{j,1}\check{x}_{j,2}$  in Eq. (12), we regard it as a new unknown function  $\bar{f}_i(\check{x}_{j,2}) = \sum_{j=1}^N a_{ij}g_{j,1}\check{x}_{j,2}$ , where  $\check{x}_{j,2} = [a_{i1}\check{x}_{1,2}, \dots, a_{iN}\check{x}_{N,2}]^T$ . In this paper, a radial basis function (RBF) NN is employed to approximate this unknown function  $\bar{f}_i(\check{x}_{j,2})$ . The function can be expressed as  $\bar{f}_i(\check{x}_{j,2}) = \theta_i^{*T} \psi_i(\check{x}_{j,2}) + \delta_i$ , where  $\check{x}_{j,2} \in \Omega$  is the input of the network,  $\Omega$  is a compact set,  $\delta_i$  is the approximate error,  $\theta_i^{*T} = [\theta_{i,1}, \theta_{i,2}, \dots, \theta_{i,l}]^T \in \mathbb{R}^l$  is the ideal network weight,  $\psi_i(\check{x}_{j,2}) = [\psi_{i,1}(\check{x}_{j,2}), \psi_{i,2}(\check{x}_{j,2}), \dots, \psi_{i,l}(\check{x}_{j,2})]^T \in \mathbb{R}^l$  is the basis function, and  $l$  is the number of network nodes. The basis function is selected as the Gaussian function  $\psi_i(\check{x}_{j,2}) = \mu_i \exp(-||\check{x}_{j,2} - \zeta_i||^2/\pi_i^2)$ , where  $\zeta_i = [\zeta_{i1}, \zeta_{i2}, \dots, \zeta_{il}]^T$  is the center of the basis function,  $\pi_i$  is the width of the basis function, and  $\mu_i$  is the amplification factor. Now, we choose the designed virtual control law

$$\alpha_{i,2} = N_{i,1}(\kappa_{i,1}) \left[ k_{i,1}e_{i,1} - \frac{e_{i,1}\check{x}_{i,1}^2\hat{\lambda}_{i,1}}{\sqrt{(e_{i,1}\check{x}_{i,1})^2 + \sigma_{i,1}^2}} - \frac{e_{i,1}\Psi_{i,1}^2\hat{\Theta}_{i,1}}{\sqrt{(e_{i,1}\Psi_{i,1})^2 + \sigma_{i,1}^2}} + \frac{1}{d_i + b_i} \hat{\theta}_i^T \psi_i(\check{x}_{j,2}) \right. \\ \left. - \frac{1}{d_i + b_i} \frac{e_{i,1}\check{x}_{j,1}^2\hat{\lambda}_{i,1}}{\sqrt{(e_{i,1}\check{x}_{j,1})^2 + \sigma_{i,1}^2}} - \frac{1}{d_i + b_i} \frac{e_{i,1}\Psi_{j,1}^2\hat{\Theta}_{i,1}}{\sqrt{(e_{i,1}\Psi_{j,1})^2 + \sigma_{i,1}^2}} + \frac{b_i}{d_i + b_i} \dot{y}_r \right] \quad (18)$$

with

$$\dot{\kappa}_{i,1} = \left[ k_{i,1}e_{i,1} - \frac{e_{i,1}\check{x}_{i,1}^2\hat{\lambda}_{i,1}}{\sqrt{(e_{i,1}\check{x}_{i,1})^2 + \sigma_{i,1}^2}} - \frac{e_{i,1}\Psi_{i,1}^2\hat{\Theta}_{i,1}}{\sqrt{(e_{i,1}\Psi_{i,1})^2 + \sigma_{i,1}^2}} + \frac{1}{d_i + b_i} \hat{\theta}_i^T \psi_i(\check{x}_{i,2}) \right. \\ \left. - \frac{1}{d_i + b_i} \frac{e_{i,1}\check{x}_{j,1}^2\hat{\lambda}_{i,1}}{\sqrt{(e_{i,1}\check{x}_{j,1})^2 + \sigma_{i,1}^2}} - \frac{1}{d_i + b_i} \frac{e_{i,1}\Psi_{j,1}^2\hat{\Theta}_{i,1}}{\sqrt{(e_{i,1}\Psi_{j,1})^2 + \sigma_{i,1}^2}} + \frac{b_i}{d_i + b_i} \dot{y}_r \right] e_{i,1}, \quad (19)$$

and

$$\begin{cases} \dot{\hat{\lambda}}_{i,1} = (d_i + b_i) \frac{(e_{i,1}\check{x}_{i,1})^2}{\sqrt{(e_{i,1}\check{x}_{i,1})^2 + \sigma_{i,1}^2}} - q_{i,1}\hat{\lambda}_{i,1}, \\ \dot{\underline{\lambda}}_{i,1} = -\frac{(e_{i,1}\check{x}_{j,1})^2}{\sqrt{(e_{i,1}\check{x}_{j,1})^2 + \sigma_{i,1}^2}} - p_{i,1}\hat{\underline{\lambda}}_{i,1}, \\ \dot{\hat{\Theta}}_{i,1} = (d_i + b_i) \frac{(e_{i,1}\Psi_{i,1})^2}{\sqrt{(e_{i,1}\Psi_{i,1})^2 + \sigma_{i,1}^2}} - \underline{q}_{i,1}\hat{\Theta}_{i,1}, \\ \dot{\underline{\Theta}}_{i,1} = -\frac{(e_{i,1}\Psi_{j,1})^2}{\sqrt{(e_{i,1}\Psi_{j,1})^2 + \sigma_{i,1}^2}} - p_{i,1}\hat{\underline{\Theta}}_{i,1}, \\ \dot{\hat{\theta}}_i = \Gamma_i [\psi_i(\check{x}_{j,2})e_{i,1} - \gamma_i\hat{\theta}_i], \end{cases} \quad (20)$$

where  $N_{i,1}(\kappa_{i,1})$  is a Nussbaum function,  $\kappa_{i,1}$  is the input of  $N_{i,1}(\cdot)$ ,  $k_{i,1}$ ,  $\Gamma_i$ ,  $\sigma_{i,1}$ ,  $q_{i,1}$ ,  $\underline{q}_{i,1}$ ,  $p_{i,1}$  and  $\underline{p}_{i,1}$  are the adjustable control parameters, and  $\hat{\theta}_i$ ,  $\hat{\lambda}_{i,1}$ ,  $\hat{\Theta}_{i,1}$ ,  $\underline{\lambda}_{i,1}$  and  $\underline{\Theta}_{i,1}$  are attack adaptive compensation parameters for estimation of  $\theta_i^*$ ,  $\lambda_{i,1}^*$ ,  $\Theta_{i,1}^*$ ,  $\underline{\lambda}_{i,1}^*$  and  $\underline{\Theta}_{i,1}^*$ , respectively.

From the DSC technique, we introduce a first-order filter

$$\tau_{i,2}\dot{z}_{i,2} + z_{i,2} = \alpha_{i,2} \quad (21)$$

with  $z_{i,2}(0) = \alpha_{i,2}(0)$ , where  $\tau_{i,2}$  is a positive time constant.

Choose a Lyapunov function candidate

$$V_{i,1} = \sum_{i=1}^N \left( \frac{1}{2} e_{i,1}^2 + \frac{1}{2} \tilde{\lambda}_{i,1}^2 + \frac{1}{2} \tilde{\Theta}_{i,1}^2 + \frac{1}{2} \tilde{\lambda}_{i,1}^2 + \frac{1}{2} \tilde{\Theta}_{i,1}^2 + \frac{1}{2} \tilde{\theta}_i^T \Gamma_i^{-1} \tilde{\theta}_i \right), \quad (22)$$

where  $\tilde{\lambda}_{i,1} = \underline{\lambda}_{i,1}^* - \hat{\lambda}_{i,1}$ ,  $\tilde{\Theta}_{i,1} = \underline{\Theta}_{i,1}^* - \hat{\Theta}_{i,1}$ ,  $\tilde{\lambda}_{j,1} = \lambda_{j,1}^* - \hat{\lambda}_{j,1}$ ,  $\tilde{\Theta}_{j,1} = \Theta_{j,1}^* - \hat{\Theta}_{j,1}$ , and  $\tilde{\theta}_i = \theta_i^* - \hat{\theta}_i$ . The derivative of  $V_{i,1}$  with (12)-(17) and (20) is

$$\begin{aligned} \dot{V}_{i,1} &\leq \sum_{i=1}^N \left\{ (d_i + b_i) \left[ g_{i,1}e_{i,1}\alpha_{i,2} + \frac{(e_{i,1}\check{x}_{i,1})^2 \lambda_{i,1}^*}{\sqrt{(e_{i,1}\check{x}_{i,1})^2 + \sigma_{i,1}^2}} + \frac{(e_{i,1}\Psi_{i,1})^2 \Theta_{i,1}^*}{\sqrt{(e_{i,1}\Psi_{i,1})^2 + \sigma_{i,1}^2}} - \frac{1}{d_i + b_i} \theta_i^{*T} \psi(\check{x}_{j,2})e_{i,1} \right. \right. \\ &\quad \left. \left. + \frac{1}{d_i + b_i} \frac{(e_{i,1}\check{x}_{j,1})^2 \lambda_{i,1}^*}{\sqrt{(e_{i,1}\check{x}_{j,1})^2 + \sigma_{i,1}^2}} + \frac{1}{d_i + b_i} \frac{(e_{i,1}\Psi_{j,1})^2 \Theta_{i,1}^*}{\sqrt{(e_{i,1}\Psi_{j,1})^2 + \sigma_{i,1}^2}} + \frac{b_i}{d_i + b_i} e_{i,1} \dot{y}_r \right] \right. \\ &\quad + (d_i + b_i)g_{i,1}e_{i,1}(e_{i,2} + \varpi_{i,2}) - (d_i + b_i) \left( \frac{(e_{i,1}\check{x}_{i,1})^2 \tilde{\lambda}_{i,1}}{\sqrt{(e_{i,1}\check{x}_{i,1})^2 + \sigma_{i,1}^2}} + \frac{(e_{i,1}\Psi_{i,1})^2 \tilde{\Theta}_{i,1}}{\sqrt{(e_{i,1}\Psi_{i,1})^2 + \sigma_{i,1}^2}} \right) \\ &\quad - \tilde{\theta}_i^T \left[ \psi_i(\check{x}_{j,2})e_{i,1} - \sigma_i\hat{\theta}_i \right] + \frac{(e_{i,1}\check{x}_{j,1})^2 \tilde{\lambda}_{i,1}}{\sqrt{(e_{i,1}\check{x}_{j,1})^2 + \sigma_{i,1}^2}} + \frac{(e_{i,1}\Psi_{j,1})^2 \tilde{\Theta}_{i,1}}{\sqrt{(e_{i,1}\Psi_{j,1})^2 + \sigma_{i,1}^2}} + q_{i,1}\tilde{\lambda}_{i,1}\hat{\lambda}_{i,1} + \underline{q}_{i,1}\tilde{\Theta}_{i,1}\hat{\Theta}_{i,1} \right. \\ &\quad \left. + e_{i,1}\delta_i + (d_i + b_i)(\lambda_{i,1}^*\sigma_{i,1} + \Theta_{i,1}^*\sigma_{i,1} + \underline{\lambda}_{i,1}^*\sigma_{i,1} + \underline{\Theta}_{i,1}^*\sigma_{i,1}) + p_{i,1}\tilde{\lambda}_{i,1}\hat{\lambda}_{i,1} + \underline{p}_{i,1}\tilde{\Theta}_{i,1}\hat{\Theta}_{i,1} \right\}. \end{aligned} \quad (23)$$

Then, substituting the virtual control law (18) into (23) and combining with the given Nussbaum function input update law (19), we rewrite (23) as

$$\begin{aligned} \dot{V}_{i,1} &\leq \sum_{i=1}^N \left\{ (d_i + b_i)g_{i,1}(x_{i,1})N_{i,1}(\kappa_{i,1})\dot{k}_{i,1} + (d_i + b_i)\dot{k}_{i,1} + \sigma_i\tilde{\theta}_i^T\hat{\theta}_i \right. \\ &\quad - (d_i + b_i)k_{i,1}^2 + (d_i + b_i)g_{i,1}(x_{i,1})e_{i,1}(e_{i,2} + \varpi_{i,2}) + e_{i,1}\delta_i \\ &\quad \left. + (d_i + b_i)(\lambda_{i,1}^*\sigma_{i,1} + \Theta_{i,1}^*\sigma_{i,1} + \underline{\lambda}_{i,1}^*\sigma_{i,1} + \underline{\Theta}_{i,1}^*\sigma_{i,1}) + p_{i,1}\tilde{\lambda}_{i,1}\hat{\lambda}_{i,1} + \underline{p}_{i,1}\tilde{\Theta}_{i,1}\hat{\Theta}_{i,1} + q_{i,1}\tilde{\lambda}_{i,1}\hat{\lambda}_{i,1} + \underline{q}_{i,1}\tilde{\Theta}_{i,1}\hat{\Theta}_{i,1} \right\}. \end{aligned} \quad (24)$$

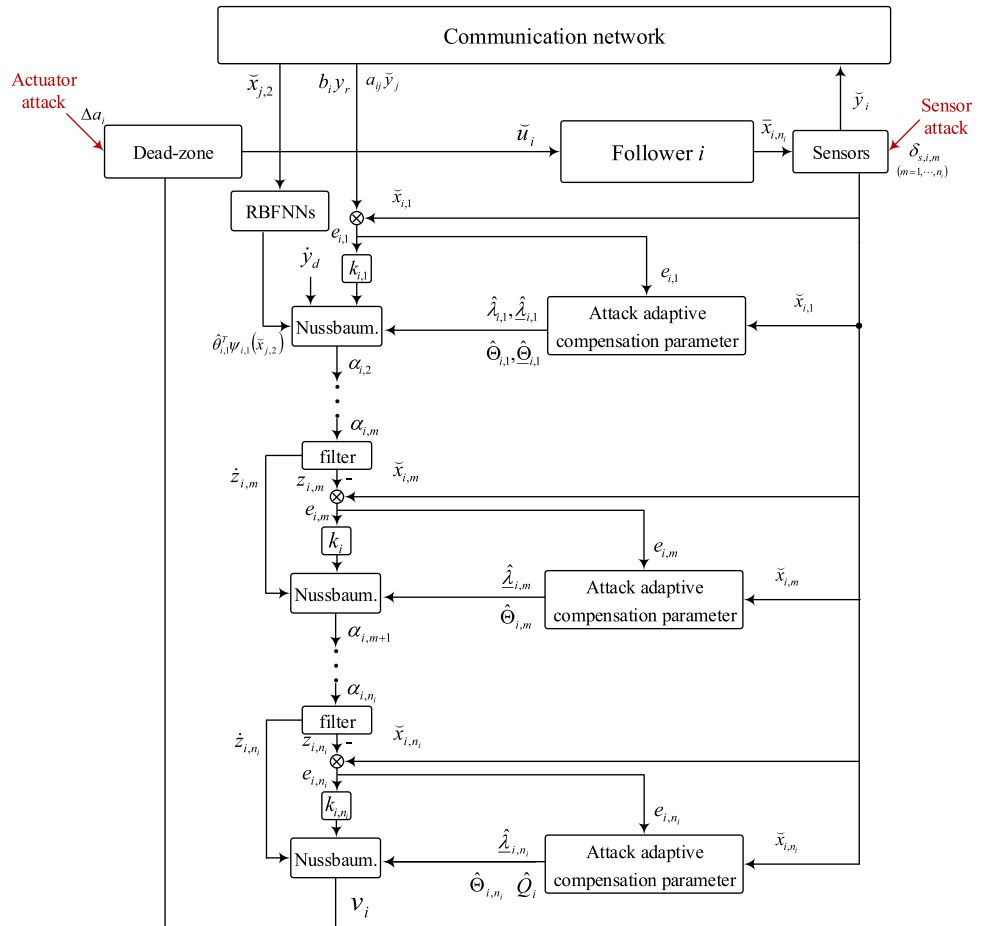
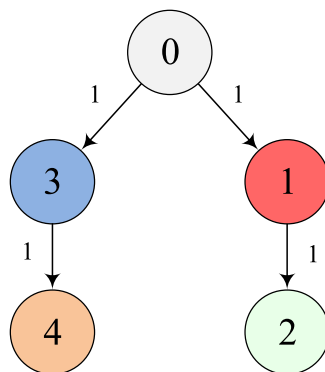
Fig. 3. The structure of secure control strategy for the  $i$ th follower.

Fig. 4. Communication topology in Example A.

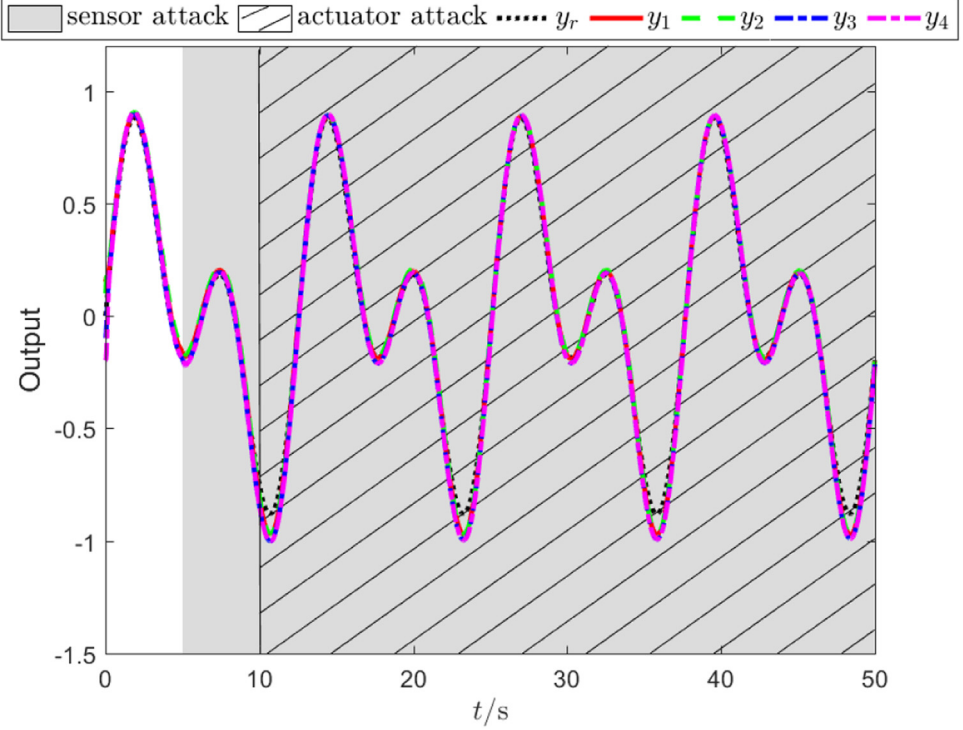


Fig. 5. Trajectories of the leader and followers in Example A.

Due to the existance of  $g_{i,1}(x_{i,1})e_{i,1}e_{i,2}$  in Eq. (23), the Lemma 1 can not be applied directly. We have to deal with the item in next step.

**Step m** ( $m = 2, \dots, n_i - 1$ ): Considering (9) and the  $i, m$ th dynamics of a follower (7), we obtain

$$e_{i,m}\dot{e}_{i,m} = e_{i,m}\dot{\lambda}_{i,m}\lambda_{i,m}^{-1}\ddot{x}_{i,m} + g_{i,m}(\bar{x}_{i,m})e_{i,m}\ddot{x}_{i,m+1} + \lambda_{i,m}f_{i,m}(\bar{x}_{i,m})e_{i,m} - e_{i,m}\dot{z}_{i,m}. \quad (25)$$

Applying Lemma 3 and Assumption 3, we have

$$e_{i,m}\dot{\lambda}_{i,m}\lambda_{i,m}^{-1}\ddot{x}_{i,m} \leq \lambda_{i,m}^*\left(\sigma_{i,m} + \frac{(e_{i,m}\ddot{x}_{i,m})^2}{\sqrt{(e_{i,m}\ddot{x}_{i,m})^2 + \sigma_{i,m}^2}}\right). \quad (26)$$

Similarly, because the states in a follower are paralyzed by sensor attack and their original states are not available, the function  $f_{i,m}(\bar{x}_{i,m})$  needs to be separated. Substituting  $\ddot{x}_{i,m} = \lambda_{i,m}x_{i,m}$  in Eq. (25), it results  $|f_{i,m}(\bar{x}_{i,m})| = |\lambda_{i,m}^{-1}\ddot{x}_{i,m}|$ . From Lemma 2, there exist two smooth functions  $w_{i,m}(\cdot)$  and  $\Psi_{i,m}(\cdot)$  and an unknown positive constant  $\bar{w}_{i,m}$  satisfying  $w_{i,m}(\lambda_{i,m}^{-1}) \leq \bar{w}_{i,m}$  such that

$$\begin{aligned} |f_{i,m}(\bar{x}_{i,m})| &= \left|f_{i,m}\left(\lambda_{i,m}^{-1}\ddot{x}_{i,m}\right)\right| \\ &\leq w_{i,m}(\lambda_{i,m}^{-1})\Psi_{i,m}(\ddot{x}_{i,m}) \end{aligned}$$

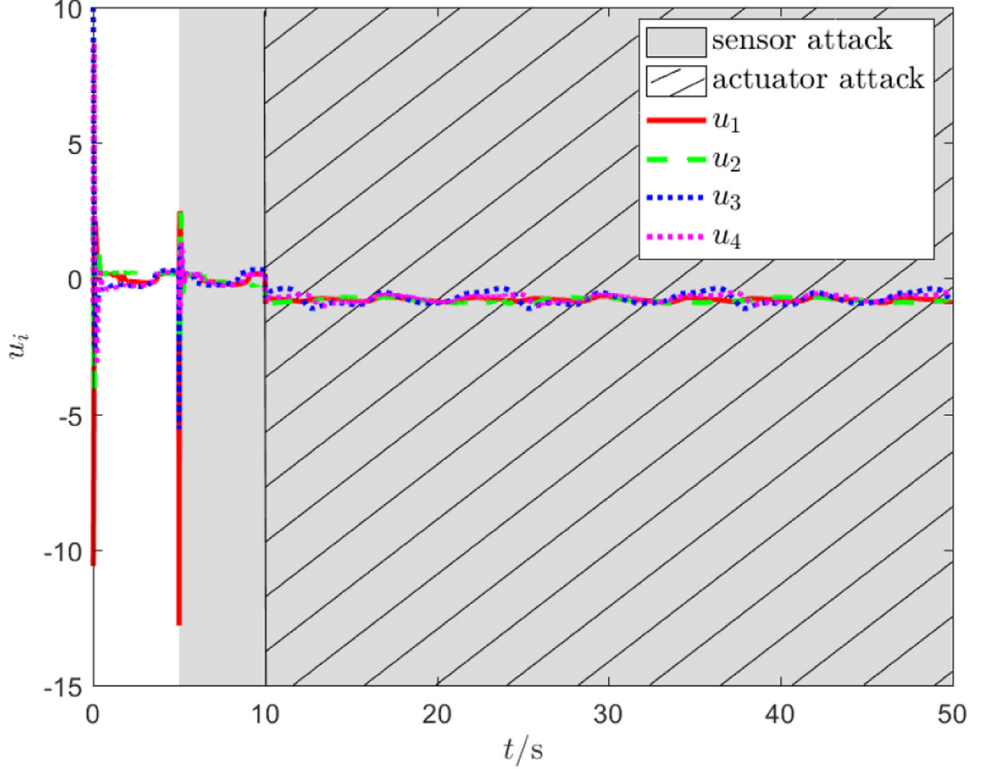


Fig. 6. Control inputs of followers in Example A.

$$\leq \bar{w}_{i,m} \Psi_{i,m}(\check{x}_{i,m}). \quad (27)$$

Denote  $\Theta_{i,m}^* = \bar{w}_{i,m} \lambda_{i,m}$ . Applying Lemma 3, Assumption 3 and Eq. (27), we have

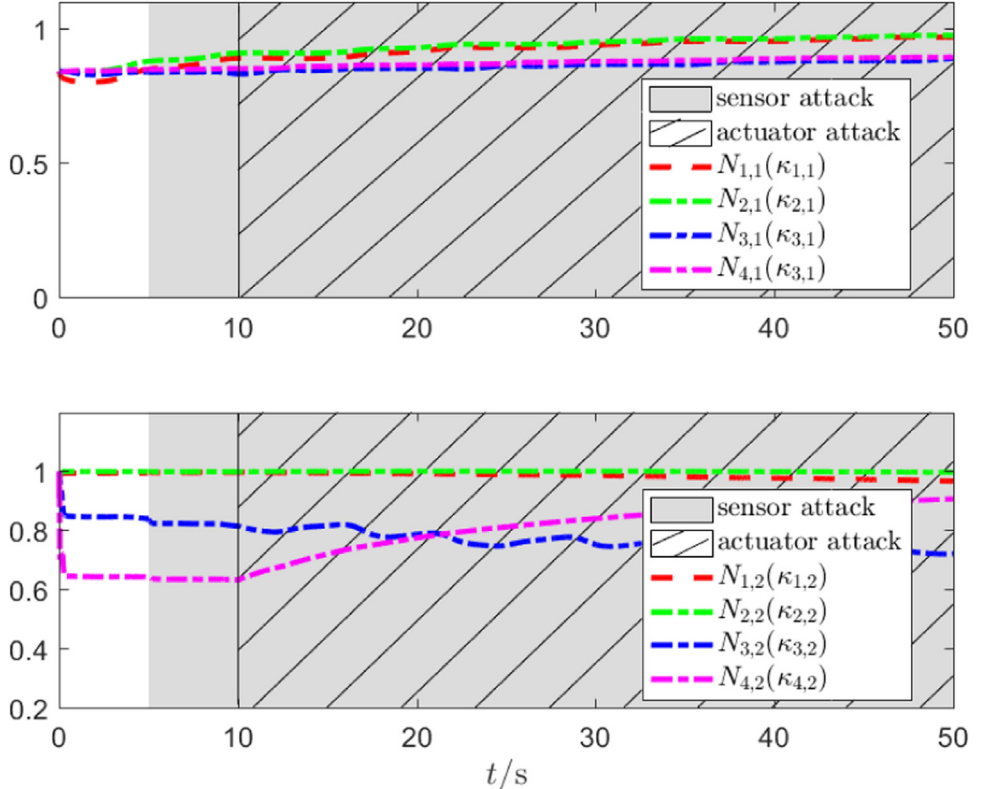
$$e_{i,m} \lambda_{i,m} f_{i,m}(\bar{x}_{i,m}) \leq \Theta_{i,m}^* \left( \sigma_{i,m} + \frac{(e_{i,m} \Psi_{i,m})^2}{\sqrt{(e_{i,m} \Psi_{i,m})^2 + \sigma_{i,m}^2}} \right). \quad (28)$$

The virtual control law of this step is chosen as

$$\alpha_{i,m+1} = N_{i,m}(\kappa_{i,m}) \left[ k_{i,m} e_{i,m} - \frac{e_{i,m} \check{x}_{i,m}^2 \hat{\lambda}_{i,m}}{\sqrt{(e_{i,m} \check{x}_{i,m})^2 + \sigma_{i,m}^2}} - \frac{e_{i,m} \Psi_{i,m}^2 \hat{\Theta}_{i,m}}{\sqrt{(e_{i,m} \Psi_{i,m})^2 + \sigma_{i,m}^2}} + \dot{z}_{i,m} \right] \quad (29)$$

with

$$\begin{cases} \dot{\hat{\lambda}}_{i,m} = \frac{(e_{i,m} \check{x}_{i,m})^2}{\sqrt{(e_{i,m} \check{x}_{i,m})^2 + \sigma_{i,m}^2}} - q_{i,m} \hat{\lambda}_{i,m} \\ \dot{\hat{\Theta}}_{i,m} = \frac{(e_{i,m} \Psi_{i,m})^2}{\sqrt{(e_{i,m} \Psi_{i,m})^2 + \sigma_{i,m}^2}} - q_{i,m} \hat{\Theta}_{i,m} \end{cases} \quad (30)$$

Fig. 7. Nussbaum function  $N_{i,j}(\kappa_{i,j})$  in Example A.

and

$$\dot{\kappa}_{i,m} = \left( k_{i,m} e_{i,m} - \frac{e_{i,m} \ddot{x}_{i,m}^2 \hat{\lambda}_{i,m}}{\sqrt{(e_{i,m} \ddot{x}_{i,m})^2 + \sigma_{i,m}^2}} - \frac{e_{i,m} \Psi_{i,m}^2 \hat{\Theta}_{i,m}}{\sqrt{(e_{i,m} \Psi_{i,m})^2 + \sigma_{i,m}^2}} + \dot{z}_{i,m} \right) e_{i,m}, \quad (31)$$

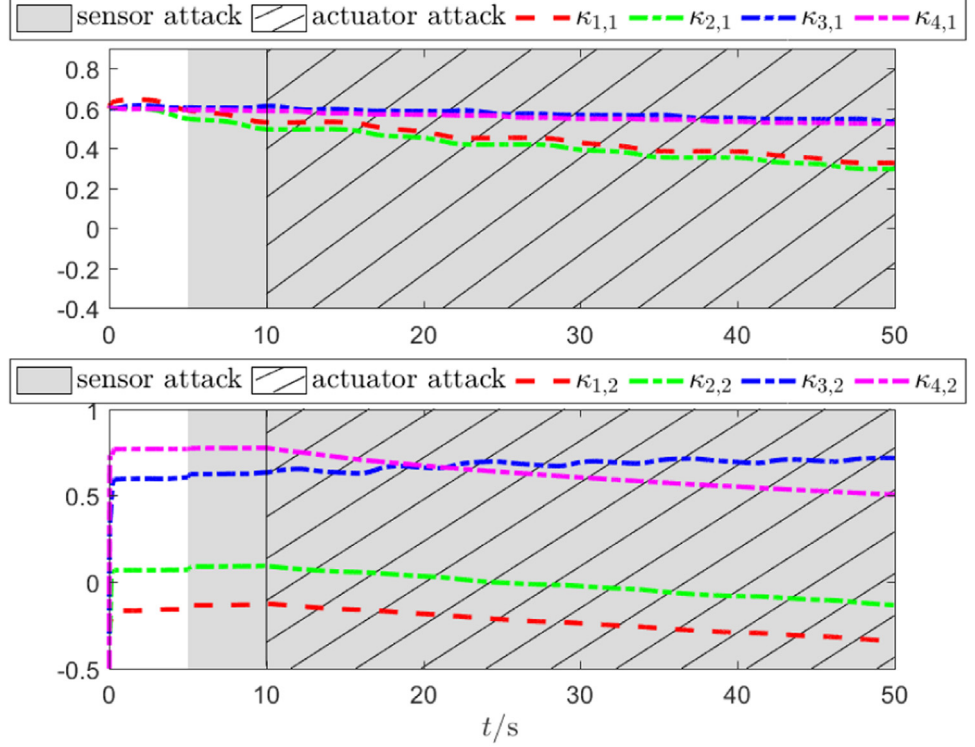
where  $N_{i,m}(\kappa_{i,m})$  is a Nussbaum function,  $\kappa_{i,m}$  is the input of the Nussbaum function,  $k_{i,m}$ ,  $\sigma_{i,m}$ ,  $q_{i,m}$  and  $\underline{q}_{i,m}$  are the adjustable control parameters, and  $\hat{\lambda}_{i,m}$  and  $\hat{\Theta}_{i,m}$  are estimations of  $\lambda_{i,m}^*$  and  $\Theta_{i,m}^*$ , respectively.

A first-order filter is introduced to obtain a filtered signal for the virtual control law  $\alpha_{i,m+1}$  by

$$\tau_{i,m+1} \dot{z}_{i,m+1} + z_{i,m+1} = \alpha_{i,m+1}, \quad z_{i,m+1}(0) = \alpha_{i,m+1}(0) \quad (32)$$

where  $\tau_{i,m+1}$  is a positive time constant.

**Remark 7.** For sensor attacks, a function separation theorem is introduced to separate attack signals, and adaptive learning parameters are introduced to compensate them. In the item  $e_{i,m} \dot{e}_{i,m}$ , there exist attack-related items  $e_{i,m} \dot{\lambda}_{i,m} \lambda_{i,m}^{-1} \ddot{x}_{i,m}$  and  $\lambda_{i,m} f_{i,m}(\bar{x}_{i,m}) e_{i,m}$ . Applying Lemma 3 and Assumption 3, we separate the information related to the upper bound of the attack  $\lambda_{i,m}^*$  and  $\Theta_{i,m}^*$  from  $e_{i,m} \dot{\lambda}_{i,m} \lambda_{i,m}^{-1} \ddot{x}_{i,m}$  and  $\lambda_{i,m} f_{i,m}(\bar{x}_{i,m}) e_{i,m}$ , respectively. We then construct

Fig. 8. Adaptive parameters  $\kappa_{i,j}$  in Example A.

corresponding adaptive parameters  $\hat{\lambda}_{i,m}$  and  $\hat{\Theta}_{i,m}$  and introduce them into control laws. They compensate for the impact of malicious attacks on error dynamics  $e_{i,m}$  and alleviate influence of attacks on an MAS.

Choose a Lyapunov function candidate

$$V_{i,m} = \sum_{i=1}^N \left( \frac{1}{2} e_{i,m}^2 + \frac{1}{2} \tilde{\lambda}_{i,m}^2 + \frac{1}{2} \tilde{\Theta}_{i,m}^2 \right), \quad (33)$$

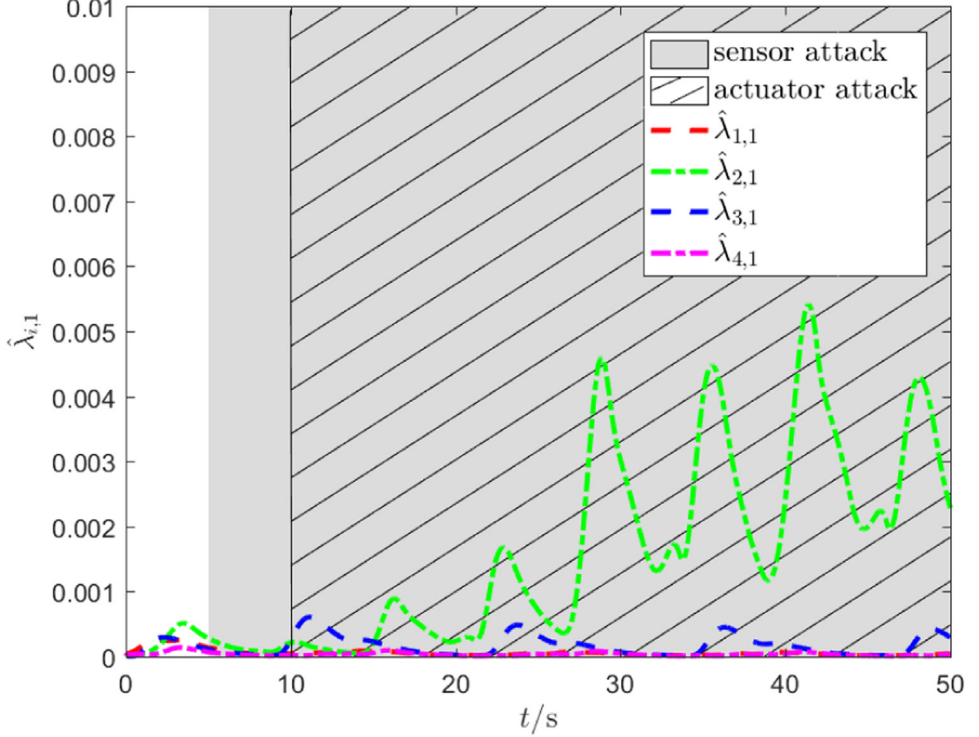
where  $\tilde{\lambda}_{i,m} = \lambda_{i,m}^* - \hat{\lambda}_{i,m}$ ,  $\tilde{\Theta}_{i,m} = \Theta_{i,m}^* - \hat{\Theta}_{i,m}$ . Taking the derivative of  $V_{i,m}$  and combining the derivative of  $e_{i,m}$ , virtual control law (29) and the update laws (30),(31), we obtain

$$\begin{aligned} \dot{V}_{i,m} \leq & \sum_{i=1}^N \left[ g_{i,m}(\bar{x}_{i,m}) N_{i,m}(\kappa_{i,m}) \dot{\kappa}_{i,m} + \dot{\kappa}_{i,m} - k_{i,m} e_{i,m}^2 + g_{i,m}(\bar{x}_{i,m}) e_{i,m} (e_{i,m+1} + \varpi_{i,m+1}) \right. \\ & \left. + q_{i,m} \tilde{\lambda}_{i,m} \hat{\lambda}_{i,m} + q_{i,m} \tilde{\Theta}_{i,m} \hat{\Theta}_{i,m} + \lambda_{i,m}^* \sigma_{i,m} + \Theta_{i,m}^* \sigma_{i,m} \right]. \end{aligned} \quad (34)$$

Similarly, due to the item  $g_{i,m}(\bar{x}_{i,m}) e_{i,m} e_{i,m+1}$ , the Lemma 1 can not be applied to Eq. (34) directly. Now we give the final design step.

**Step  $n_i$ :** From surface error (7) and the dynamic of follower (9), it follows that

$$e_{i,n_i} \dot{e}_{i,n_i} = e_{i,n_i} \dot{\lambda}_{i,n_i} \lambda_{i,n_i}^{-1} \ddot{x}_{i,n_i} + \lambda_{i,n_i} g_{i,n_i}(\bar{x}_{i,n_i}) e_{i,n_i} \ddot{u}_i + \lambda_{i,n_i} f_{i,n_i}(\bar{x}_{i,n_i}) e_{i,n_i} - e_{i,n_i} \dot{z}_{i,n_i}. \quad (35)$$

Fig. 9. Adaptive parameters  $\hat{\lambda}_{i,1}$  in Example A.

Similar to Step  $m$ , applying Lemma 2, Lemma 3 and Assumption 3, we get

$$e_{i,n_i} \dot{\lambda}_{i,n_i} \lambda_{i,n_i}^{-1} \ddot{x}_{i,n_i} \leq \lambda_{i,n_i}^* \left( \sigma_{i,n_i} + \frac{(e_{i,n_i} \ddot{x}_{i,n_i})^2}{\sqrt{(e_{i,n_i} \ddot{x}_{i,n_i})^2 + \sigma_{i,n_i}^2}} \right) \quad (36)$$

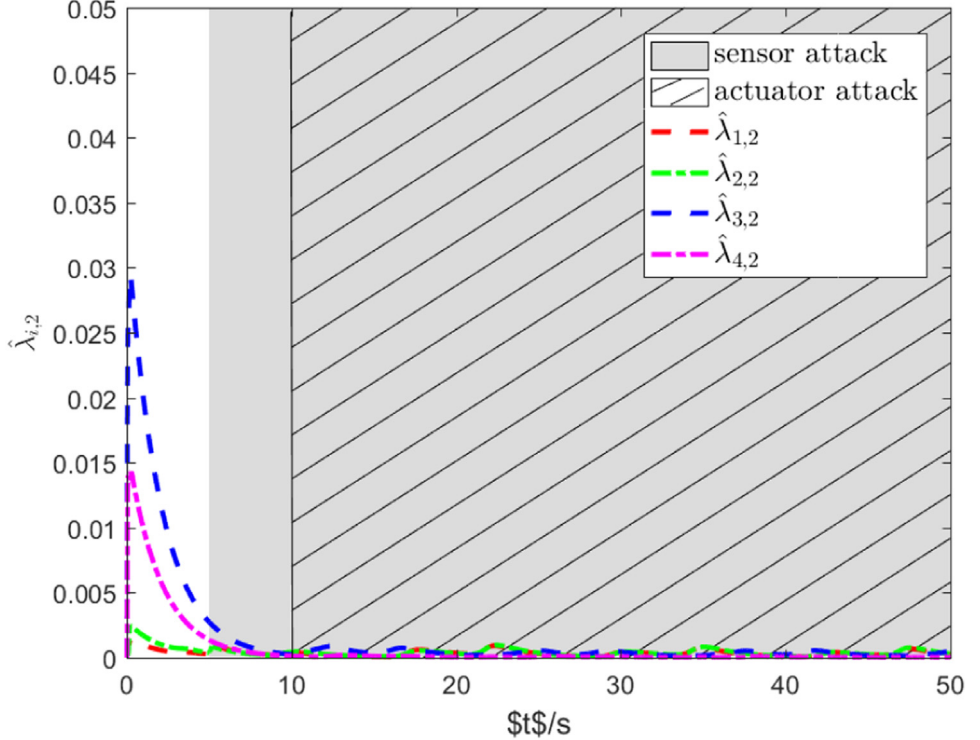
and

$$e_{i,n_i} \lambda_{i,n_i} f_{i,n_i}(x_{i,n_i}) \leq \Theta_{i,n_i}^* \left( \sigma_{i,n_i} + \frac{(e_{i,n_i} \Psi_{i,n_i})^2}{\sqrt{(e_{i,n_i} \Psi_{i,n_i})^2 + \sigma_{i,n_i}^2}} \right), \quad (37)$$

where  $\Theta_{i,n_i}^* = \bar{w}_{i,n_i} \lambda_{i,n_i}$ .

Choose the input of the dead-zone  $v_i$  as

$$v_i = N_{i,n_i}(\kappa_{i,n_i}) \left[ k_{i,n_i} e_{i,n_i} - \frac{e_{i,n_i} \ddot{x}_{i,n_i}^2 \hat{\lambda}_{i,n_i}}{\sqrt{(e_{i,n_i} \ddot{x}_{i,n_i})^2 + \sigma_{i,n_i}^2}} - \frac{e_{i,n_i} \Psi_{i,n_i}^2 \hat{\Theta}_{i,n_i}}{\sqrt{(e_{i,n_i} \Psi_{i,n_i})^2 + \sigma_{i,n_i}^2}} - \frac{e_{i,n_i} \hat{Q}_i}{\sqrt{(e_{i,n_i})^2 + \sigma_{i,n_i}^2}} + \dot{z}_{i,n_i} \right], \quad (38)$$

Fig. 10. Adaptive parameters  $\hat{\lambda}_{i,2}$  in Example A.

with

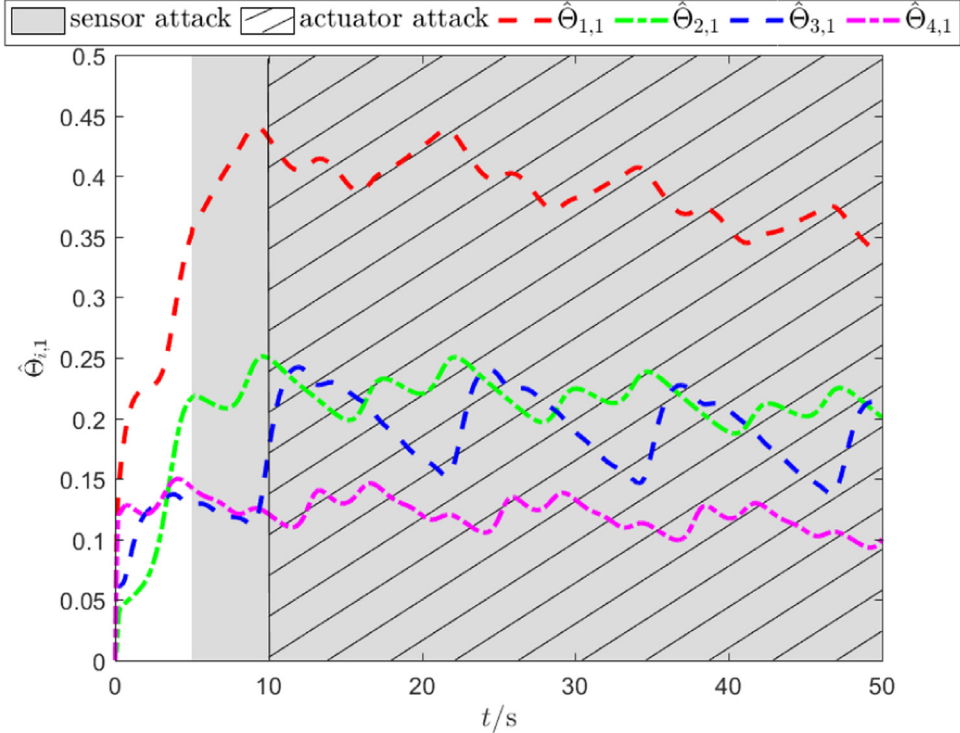
$$\begin{cases} \dot{\hat{\lambda}}_{i,n_i} = \frac{(e_{i,n_i}\check{x}_{i,n_i})^2}{\sqrt{(e_{i,n_i}\check{x}_{i,n_i})^2 + \sigma_{i,n_i}^2}} - q_{i,n_i}\hat{\lambda}_{i,n_i}, \\ \dot{\hat{\Theta}}_{i,n_i} = \frac{(e_{i,n_i}\Psi_{i,n_i})^2}{\sqrt{(e_{i,n_i}\Psi_{i,n_i})^2 + \sigma_{i,n_i}^2}} - \underline{q}_{i,n_i}\hat{\Theta}_{i,n_i}, \\ \dot{\hat{Q}}_i = \frac{(e_{i,n_i})^2}{\sqrt{(e_{i,n_i})^2 + \sigma_{i,n_i}^2}} - l_i\hat{Q}_i, \end{cases} \quad (39)$$

and

$$\dot{k}_{i,n_i} = \left( k_{i,n_i}e_{i,n_i} - \frac{e_{i,n_i}\check{x}_{i,n_i}^2\hat{\lambda}_{i,n_i}}{\sqrt{(e_{i,n_i}\check{x}_{i,n_i})^2 + \sigma_{i,n_i}^2}} - \frac{e_{i,n_i}\Psi_{i,n_i}^2\hat{\Theta}_{i,n_i}}{\sqrt{(e_{i,n_i}\Psi_{i,n_i})^2 + \sigma_{i,n_i}^2}} - \frac{e_{i,n_i}\hat{Q}_i}{\sqrt{(e_{i,n_i})^2 + \sigma_{i,n_i}^2}} + \dot{z}_{i,n_i} \right) e_{i,n_i}, \quad (40)$$

where  $N_{i,n_i}(\kappa_{i,n_i})$  is the Nussbaum function,  $\kappa_{i,n_i}$  is the input of the Nussbaum function,  $k_{i,n_i}$ ,  $q_{i,n_i}$ ,  $\underline{q}_{i,n_i}$  and  $l_i$  are the adjustable control parameters,  $\hat{\lambda}_{i,n_i}$ ,  $\hat{\Theta}_{i,n_i}$  and  $\hat{Q}_i$  are estimates of  $\lambda_{i,n_i}^*$ ,  $\Theta_{i,n_i}^*$  and  $Q_i^*$ , respectively, and  $Q_i^*$  will be explained later.

From the recursive steps, the block diagram of the secure control strategy for the  $i$ th follower is summarized in Fig. 3.

Fig. 11. Adaptive parameters  $\hat{\Theta}_{i,1}$  in Example A.

#### 4. Stability analysis

The main result about our proposed secure consensus control strategy is summarized below.

**Theorem 1.** Consider a nonlinear MAS with followers (1) under sensor and actuator attacks (4) and (6) satisfying Assumption 1–Assumption 6, where each follower with unknown control directions and dead-zone input. For bounded initial condition, satisfying  $\{\sum_{i=1}^N [\sum_{m=1}^{n_i} (e_{i,m}^2(0) + \tilde{\lambda}_{i,m}^2(0) + \tilde{\Theta}_{i,m}^2(0)) + \tilde{\lambda}_{i,1}^2(0) + \tilde{\Theta}_{i,1}^2(0) + \tilde{\theta}_i^T(0)\Gamma_i^{-1}\tilde{\theta}_i(0) + \tilde{Q}_i^2(0) + \sum_{m=1}^{n_i-1} \varpi_{i,m+1}^2(0)] \leq 2p\}$ , where  $p$  is a positive constant, the distributed secure consensus control strategy, (18)–(20), (28)–(31) and (37)–(39), steers the output  $y_i$  from each follower to achieve consensus with the trajectory  $y_r$  from the leader, and all signals in the closed-loop MAS are ultimately bounded.

**Proof.** We choose a Lyapunov function candidate

$$V = \sum_{m=1}^{n_i} V_{i,m} + V_{\varpi}, \quad (41)$$

where  $V_{\varpi} = \sum_{i=1}^N \sum_{m=1}^{n_i-1} \frac{1}{2} \varpi_{i,m+1}^2$ .

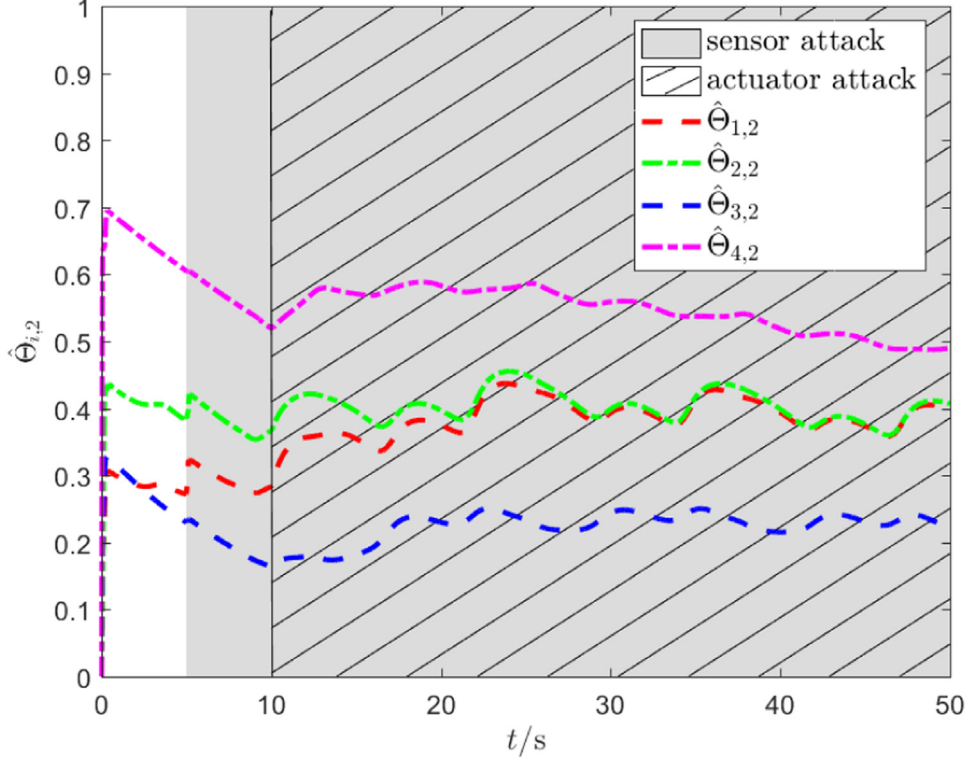


Fig. 12. Adaptive parameters  $\hat{\Theta}_{i,2}$  in Example A.

For the convenience of the proof, we first choose a Lyapunov candidate function  $V_{i,n_i}$  for Step  $n_i$

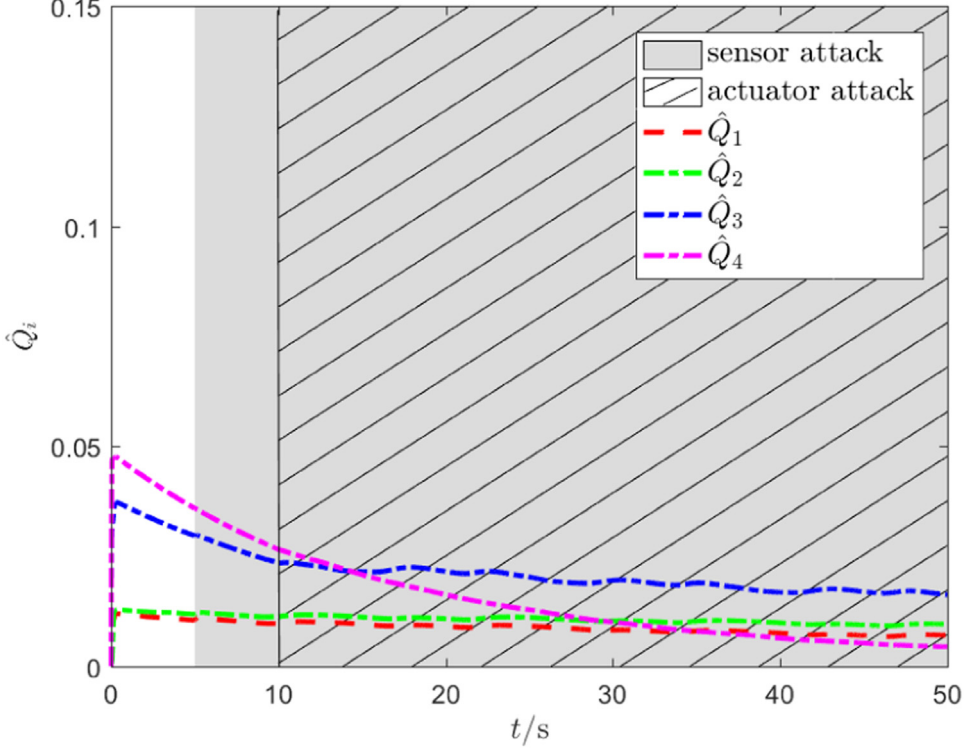
$$V_{i,n_i} = \sum_{i=1}^N \left( \frac{1}{2} e_{i,n_i}^2 + \frac{1}{2} \tilde{\lambda}_{i,n_i}^2 + \frac{1}{2} \hat{\Theta}_{i,n_i}^2 + \frac{1}{2} \tilde{Q}_i^2 \right), \quad (42)$$

where  $\tilde{\lambda}_{i,n_i} = \lambda_{i,n_i}^* - \hat{\lambda}_{i,n_i}$ ,  $\tilde{\Theta}_{i,n_i} = \Theta_{i,n_i}^* - \hat{\Theta}_{i,n_i}$ , and  $\tilde{Q}_i = Q_i^* - \hat{Q}_i$ .

Following Eqs. (35)–(37), (39), Lemma 2, Lemma 3 and Assumption 3 with (6), we obtain the time derivative of Eq. (42)

$$\begin{aligned} \dot{V}_{i,n_i} \leq & \sum_{i=1}^N \left( \left( \check{g}_{i,n_i} e_{i,n_i} v_i + \lambda_{i,n_i} g_{i,n_i} (\bar{x}_{i,n_i}) e_{i,n_i} \check{d}_i(v_i) + \frac{(e_{i,n_i} \check{x}_{i,n_i})^2 \lambda_{i,n_i}^*}{\sqrt{(e_{i,n_i} \check{x}_{i,n_i})^2 + \sigma_{i,n_i}^2}} + \frac{(e_{i,n_i} \Psi_{i,n_i})^2 \Theta_{i,n_i}^*}{\sqrt{(e_{i,n_i} \Psi_{i,n_i})^2 + \sigma_{i,n_i}^2}} \right. \right. \\ & - \frac{(e_{i,n_i} \check{x}_{i,n_i})^2 \tilde{\lambda}_{i,n_i}}{\sqrt{(e_{i,n_i} \check{x}_{i,n_i})^2 + \sigma_{i,n_i}^2}} - \frac{(e_{i,n_i} \Psi_{i,n_i})^2 \tilde{\Theta}_{i,n_i}}{\sqrt{(e_{i,n_i} \Psi_{i,n_i})^2 + \sigma_{i,n_i}^2}} - \frac{(e_{i,n_i})^2 \tilde{Q}_i}{\sqrt{(e_{i,n_i})^2 + \sigma_{i,n_i}^2}} - e_{i,n_i} \dot{z}_{i,n_i} \\ & \left. \left. + q_{i,n_i} \tilde{\lambda}_{i,n_i} \hat{\lambda}_{i,n_i} + q_{i,n_i} \tilde{\Theta}_{i,n_i} \hat{\Theta}_{i,n_i} + l_i \tilde{Q}_i \hat{Q}_i + \lambda_{i,n_i}^* \sigma_{i,n_i} + \Theta_{i,n_i}^* \sigma_{i,n_i} \right) \right), \end{aligned} \quad (43)$$

where  $\check{g}_{i,n_i} = \lambda_{i,n_i} g_{i,n_i} (\bar{x}_{i,n_i}) \bar{H}_i$  as a composite unknown control direction includes sensor attack, unknown control gain and the rake ratio of dead-zone. Applying Assumption 2,

Fig. 13. Adaptive parameters  $\hat{Q}_i$  in Example A.

**Assumption 3** and **Lemma 3**, we have

$$\lambda_{i,n_i} g_{i,n_i} (\bar{x}_{i,n_i}) e_{i,n_i} \check{d}_i \leq Q_i^* \left( \sigma_{i,n_i} + \frac{(e_{i,n_i})^2}{\sqrt{(e_{i,n_i})^2 + \sigma_{i,n_i}^2}} \right), \quad (44)$$

where  $Q_i^* = \lambda_{i,n_i} \bar{g} \check{d}_i$ . Then, following the process Eqs. (43) with (38) and (40) yields

$$\begin{aligned} \dot{V}_{i,n_i} &\leq \sum_{i=1}^N \left( \check{g}_{i,n_i} N_{i,n_i} (\kappa_{i,n_i}) \dot{x}_{i,n_i} + \dot{\kappa}_{i,n_i} - k_{i,n_i} e_{i,n_i}^2 + q_{i,n_i} \tilde{\lambda}_{i,n_i} \hat{\lambda}_{i,n_i} + \underline{q}_{i,n_i} \tilde{\Theta}_{i,n_i} \hat{\Theta}_{i,n_i} \right. \\ &\quad \left. + l_i \tilde{Q}_i \hat{Q}_i + \lambda_{i,n_i}^* \sigma_{i,n_i} + \Theta_{i,n_i}^* \sigma_{i,n_i} + Q_i^* \sigma_{i,n_i} \right). \end{aligned} \quad (45)$$

Now, taking the derivative of  $V_{\varpi}$ , from the first-order filters (21) and (32), we get

$$\begin{aligned} \dot{V}_{\varpi} &= \sum_{i=1}^N \sum_{m=1}^{n_i-1} \varpi_{i,m+1} \left( -\frac{\varpi_{i,m+1}}{\tau_{i,m+1}} - \dot{\alpha}_{i,m+1} \right) \\ &\leq \sum_{i=1}^N \sum_{m=1}^{n_i-1} \left( -\frac{\varpi_{i,m+1}^2}{\tau_{i,m+1}} + |B_{i,m+1}(\cdot) \varpi_{i,m+1}| \right), \end{aligned} \quad (46)$$

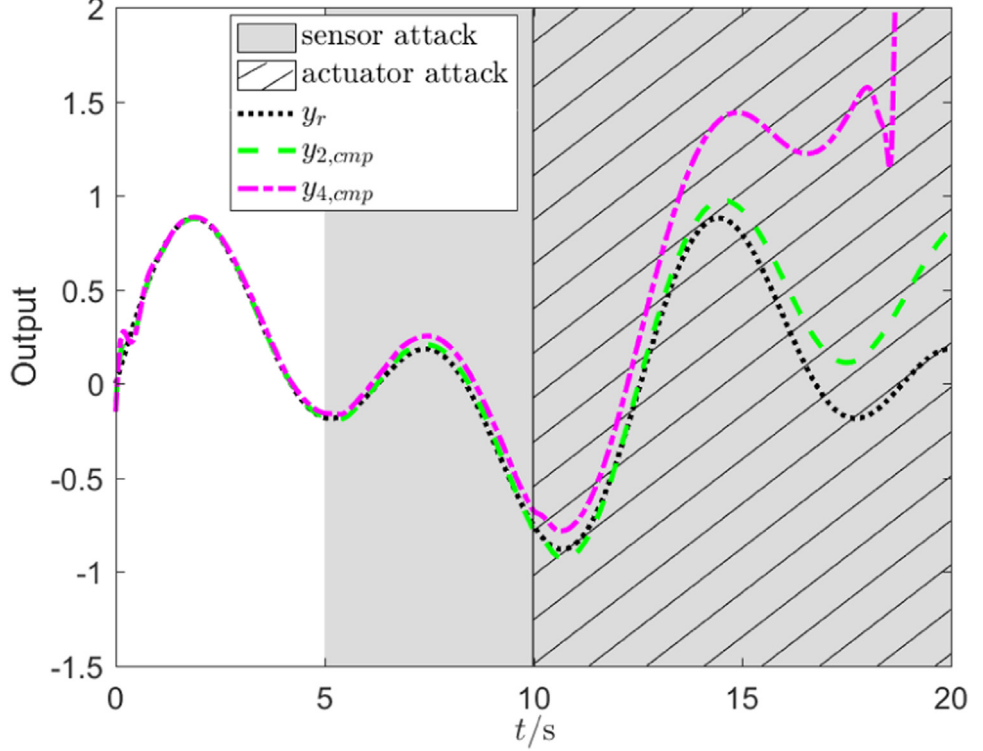


Fig. 14. Trajectories of the leader and followers with traditional consensus method [42] in Example A.

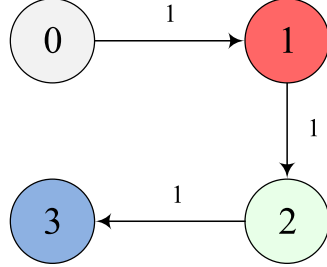


Fig. 15. Communication topology in Example B.

where  $B_{i,2}(\cdot) = \dot{\alpha}_{i,2}(e_{i,1}, e_{i,2}, z_{i,2}, \hat{\theta}_i, \check{x}_{i,1}, \check{x}_{j,1}, y_r, \dot{y}_r, \ddot{y}_r)$ ,  $j \in \Pi_i$ ,  $B_{i,m}(\cdot) = \dot{\alpha}_{i,m}(e_{i,1}, \dots, e_{i,m}, z_{i,2}, \dots, z_{i,m}, \check{x}_{i,m})$ ,  $m = 3, \dots, n_i - 1$ ,  $B_{i,n_i}(\cdot) = \dot{v}_i(e_{i,1}, \dots, e_{i,n_i}, z_{i,2}, \dots, z_{i,n_i}, \check{x}_{i,n_i})$ . It is seen that  $B_{i,m+1}(\cdot)$  is a known continuous function related to variables  $e_{i,1}, \dots, e_{i,m+1}, z_{i,2}, \dots, z_{i,m+1}, \check{x}_{i,1}, \dots, \check{x}_{i,m+1}, y_r, \dot{y}_r, \ddot{y}_r$ ,  $m = 1, \dots, n_i - 1$ .

According to Eqs. (24), (34), (45) and (46), we further obtain the time derivative of  $V$  is

$$\dot{V} \leq \sum_{i=1}^N \left\{ (d_i + b_i)(g_{i,1}N_{i,1}(\kappa_{i,1}) + 1)\dot{\kappa}_{i,1} - (d_i + b_i)k_{i,1}e_{i,1}^2 - \sum_{m=2}^{n_i} k_{i,m}e_{i,m}^2 \right\}$$

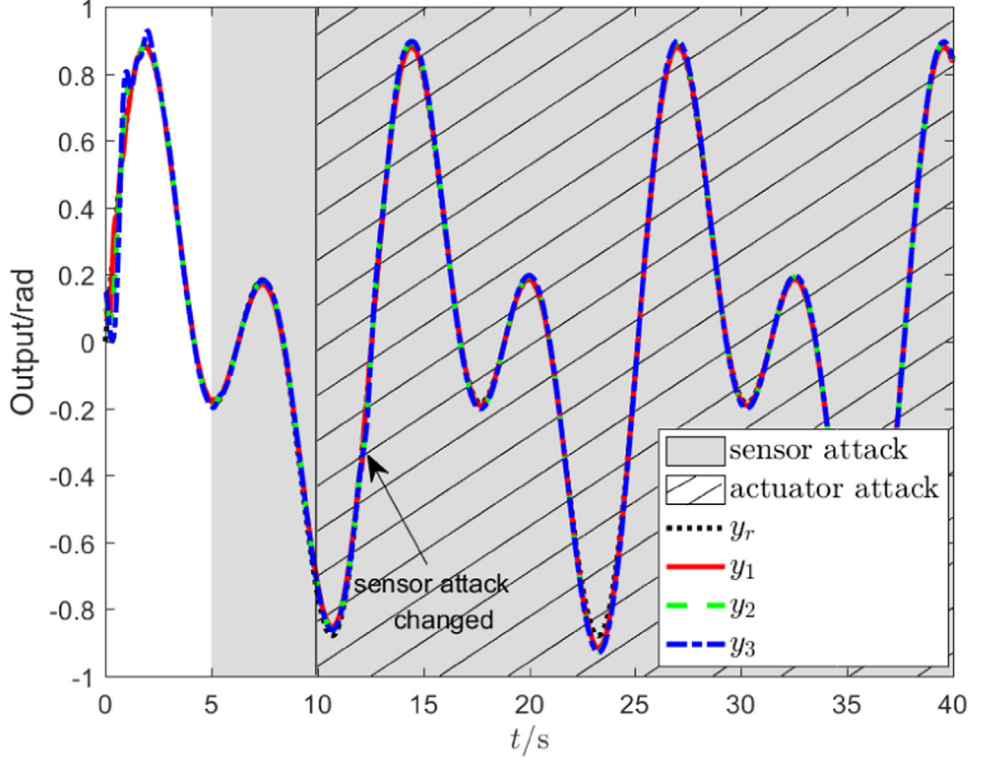


Fig. 16. Angular position trajectories of the leader and followers in Example B.

$$\begin{aligned}
& + (d_i + b_i)g_{i,1}e_{i,1}(e_{i,2} + \varpi_{i,2}) + \sum_{m=2}^{n_i-1} [g_{i,m}e_{i,m}(e_{i,m+1} + \varpi_{i,m+1}) + (g_{i,m}N_{i,m}(\kappa_{i,m}) + 1)\dot{\kappa}_{i,m}] \\
& + ((\check{g}_{i,n_i}N_{i,n_i}(\kappa_{i,n_i}) + 1)\dot{\kappa}_{i,n_i}) + \sum_{m=1}^{n_i-1} \left( -\frac{\varpi_{i,m+1}^2}{\tau_{i,m+1}} + |B_{i,m+1}(\cdot)\varpi_{i,m+1}| \right) + Q_i^*\sigma_{i,n_i} \\
& + \sigma_i\tilde{\theta}_i^T\hat{\theta}_i + p_{i,1}\tilde{\lambda}_{i,1}\hat{\lambda}_{i,1} + \underline{p}_{i,1}\tilde{\Theta}_{i,1}\hat{\Theta}_{i,1} + \sum_{m=1}^{n_i} (q_{i,m}\tilde{\lambda}_{i,m}\hat{\lambda}_{i,m} + \underline{q}_{i,m}\tilde{\Theta}_{i,m}\hat{\Theta}_{i,m}) + e_{i,1}\delta_i \\
& + \sum_{m=2}^{n_i} (\lambda_{i,m}^*\sigma_{i,m} + \Theta_{i,m}^*\sigma_{i,m}) + (d_i + b_i)(\lambda_{i,1}^*\sigma_{i,1} + \Theta_{i,1}^*\sigma_{i,1} + \underline{\lambda}_{i,1}^*\sigma_{i,1} + \underline{\Theta}_{i,1}^*\sigma_{i,1}) \}. \quad (47)
\end{aligned}$$

For any  $B_0 > 0$  and  $p > 0$ , there exist two compact sets  $\Phi_0 := \{(y_r, \dot{y}_r, \ddot{y}_r) : |y_r|^2 + |\dot{y}_r|^2 + |\ddot{y}_r|^2 \leq B_0\}$  and  $\Phi_{i,m} := \{\sum_{h=1}^m e_{i,h}^2 + \sum_{h=1}^m (\tilde{\lambda}_{i,h}^2 + \tilde{\Theta}_{i,h}^2) + \tilde{\lambda}_{i,1}^2 + \tilde{\Theta}_{i,1}^2 + \tilde{\theta}_i^T\Gamma_i^{-1}\tilde{\theta}_i + \tilde{Q}_i^2 + \sum_{h=1}^{m-1} \varpi_{i,h+1}^2 + \sum_{k \in \Pi_i} e_{k,m+1}^2 \leq 2p\}$  over  $\mathbb{R}^3$  and  $\mathbb{R}^{4m+2+\eta_i+\bar{\eta}_i}$ , respectively, where  $i = 1, \dots, N$ ,  $m = 2, \dots, n_i$ ,  $\eta_i$  is the dimension of  $\tilde{\theta}_i$ , and  $\bar{\eta}_i$  is dimension of  $\sum_{k \in \Pi_i} e_{k,m+1}^2$ . Therefore, there exists a positive constant  $\tilde{B}_{i,m+1}$  such that  $|B_{i,m+1}| \leq \tilde{B}_{i,m+1}$  over  $\Phi_0 \times \Phi_{i,m}$ .

With the Young's inequality, one has  $g_{i,m}(\bar{x}_{i,m})e_{i,m}e_{i,m+1} \leq e_{i,m}^2 + \bar{g}^2e_{i,m+1}^2/4$ ,  $g_{i,j}e_{i,m}\varpi_{i,m+1} \leq e_{i,m}^2 + \bar{g}^2\varpi_{i,m+1}^2/4$ ,  $|B_{i,m+1}\varpi_{i,m+1}| \leq \varpi_{i,m+1}^2/M_{i,m+1}^2 + M_{i,m+1}^2\tilde{B}_{i,m+1}^2$ ,  $e_{i,1}\delta_i \leq e_{i,1}^2 + \delta_i^2/4$ ,

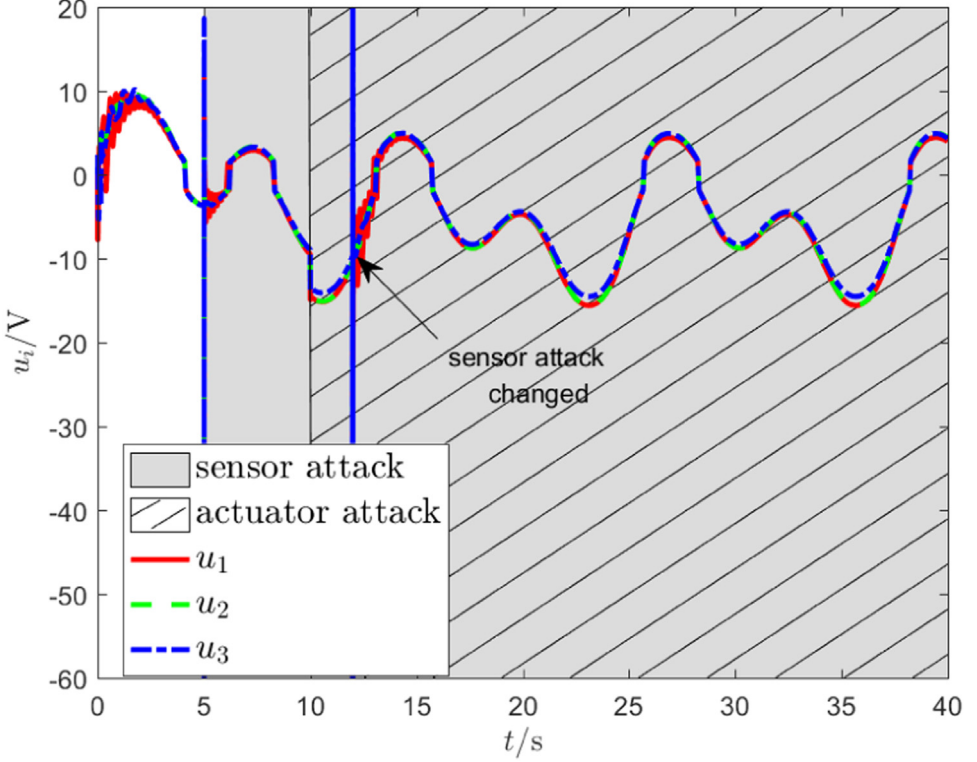
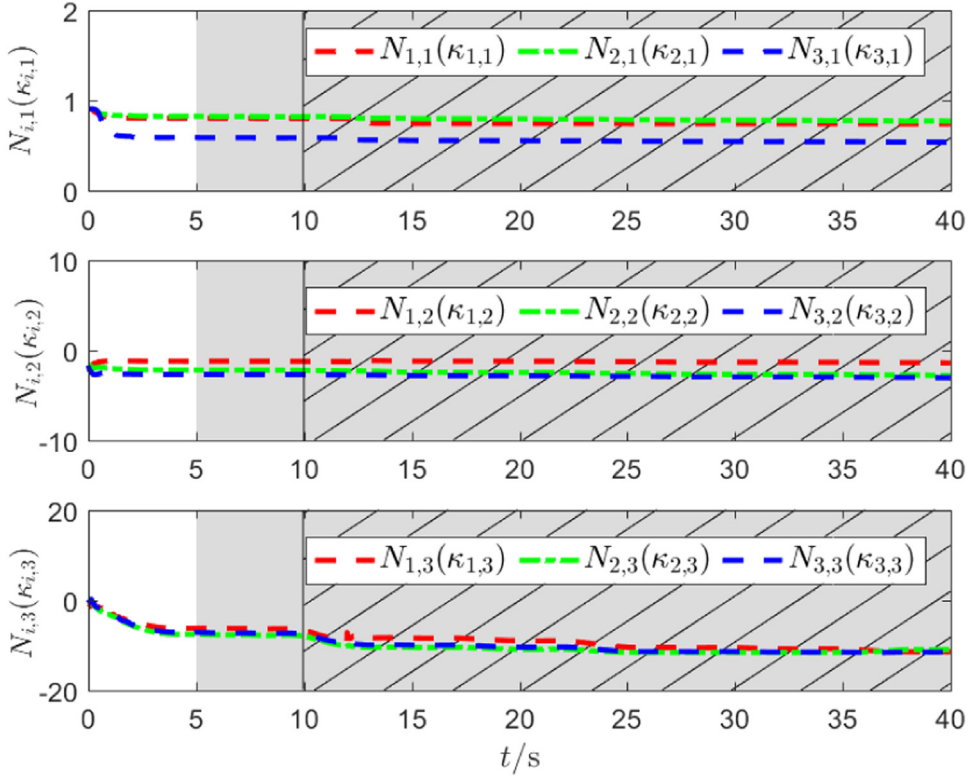


Fig. 17. Control inputs of followers in Example B.

$\tilde{\theta}_i^T \hat{\theta}_i \leq -\tilde{\theta}_i^T \tilde{\theta}_i/2 + \theta_i^{*T} \theta_i^*/2$ ,  $\tilde{\lambda}_{i,l} \hat{\lambda}_{i,1} \leq -\tilde{\lambda}_{i,1}^2/2 + \underline{\lambda}_{i,1}^{*2}/2$ ,  $\tilde{\Theta}_{i,1} \hat{\Theta}_{i,1} \leq -\tilde{\Theta}_{i,1}^2/2 + \underline{\Theta}_{i,1}^{*2}/2$ ,  $\tilde{\lambda}_{i,l} \hat{\lambda}_{i,l} \leq -\tilde{\lambda}_{i,l}^2/2 + \lambda_{i,l}^{*2}/2$  and  $\tilde{\Theta}_{i,l} \hat{\Theta}_{i,l} \leq -\tilde{\Theta}_{i,l}^2/2 + \Theta_{i,l}^{*2}/2$ , where  $M_{i,m+1} > 0$  is a constant,  $i = 1, \dots, N$ ,  $m = 1, \dots, n_i - 1$  and  $l = 1, \dots, n_i$ . Then, Eq. (47) becomes

$$\begin{aligned} \dot{V} \leq & \sum_{i=1}^N \left\{ -(d_i + b_i) \left( (k_{i,1} - 3)e_{i,1}^2 - \frac{1}{4}\bar{g}^2 e_{i,2}^2 \right) - \sum_{m=2}^{n_i-1} \left( (k_{i,m} - 2)e_{i,m}^2 + \frac{1}{4}\bar{g}^2 e_{i,m+1}^2 \right) - k_{i,n_i} e_{i,n_i}^2 \right. \\ & + \sum_{m=1}^{n_i} (\check{g}_{i,m} N_{i,m} (\kappa_{i,m}) + 1) \dot{k}_{i,m} + \left( -\frac{1}{\tau_{i,2}} + \frac{(d_i + b_i)}{4} \bar{g}^2 + \frac{1}{M_{i,2}^2} \right) \varpi_{i,2}^2 - \frac{\sigma_i}{2} \tilde{\theta}_i^T \tilde{\theta}_i \\ & - \frac{1}{2} p_{i,1} \tilde{\lambda}_{i,1}^2 - \frac{1}{2} p_{i,1} \tilde{\Theta}_{i,1}^2 \\ & \left. - \sum_{m=1}^{n_i} \left( \frac{1}{2} q_{i,m} \tilde{\lambda}_{i,m}^2 + \frac{1}{2} q_{i,m} \tilde{\Theta}_{i,m}^2 \right) - \frac{1}{2} l_i \tilde{Q}_i^2 + \sum_{m=1}^{n_i-1} \left( -\frac{1}{\tau_{i,m+1}} + \frac{1}{4} \bar{g}^2 + \frac{1}{M_{i,m+1}^2} \right) \varpi_{i,m+1}^2 \right\} + D, \end{aligned} \quad (48)$$

where  $D = \sum_{i=1}^N \left\{ \frac{\delta_i^2}{4(d_i+b_i)} + \frac{\sigma_i}{2} \theta_i^T \theta_i + \frac{p_{i,1}}{2} \underline{\lambda}_{i,1}^{*2} + \frac{p_{i,1}}{2} \underline{\Theta}_{i,1}^{*2} + \sum_{m=1}^{n_i} \left( \frac{q_{i,m}}{2} \lambda_{i,m}^{*2} + \frac{q_{i,m}}{2} \Theta_{i,m}^{*2} + \lambda_{i,m}^* \sigma_{i,m} \right) + \frac{1}{2} l_i Q_i^{*2} + \sum_{m=1}^{n_i-1} M_{i,m+1}^2 \tilde{B}_{i,m+1}^2 + (d_i + b_i) (\lambda_{i,1}^* \sigma_{i,1} + \Theta_{i,1}^* \sigma_{i,1} + \hat{\lambda}_{i,1}^* \sigma_{i,1} + \hat{\Theta}_{i,1}^* \sigma_{i,1}) + Q_i^* \sigma_{i,n_i} \right\}$ , and  $\check{g}_{i,m} = g_{i,m}$ ,  $m = 1, \dots, n_i - 1$ .

Fig. 18. Nussbaum function  $N_{i,j}(\kappa_{i,j})$  in Example B.

Select the following parameters

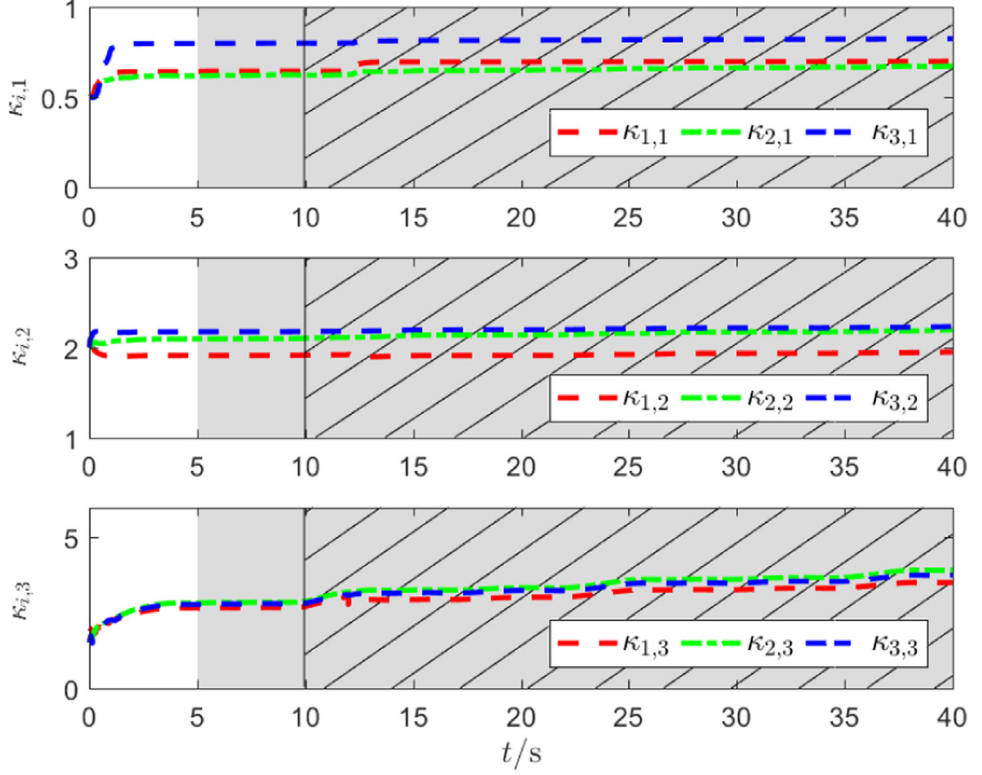
$$\begin{cases} k_{i,1} = 3 + \frac{\gamma}{d_i+b_i}, \\ k_{i,2} = 2 + \frac{d_i+b_i}{4}\bar{g}^2 + \gamma, \\ k_{i,m} = 2 + \frac{\bar{g}^2}{4} + \gamma, m = 3, \dots, n_i - 1, \\ k_{i,n_i} = \frac{\bar{g}^2}{4} + \gamma, \end{cases} \quad (49)$$

where  $\gamma \geq 0$ , and denote

$$\begin{cases} -\frac{1}{\tau_{i,2}^*} = -\frac{1}{\tau_{i,2}} + \frac{(d_i+b_i)}{4}\bar{g}^2 + \frac{1}{M_{i,2}^2}, \\ -\frac{1}{\tau_{i,m+1}^*} = -\frac{1}{\tau_{i,m+1}} + \frac{1}{4}\bar{g}^2 + \frac{1}{M_{i,m+1}^2}. \end{cases} \quad (50)$$

Using Eqs. (49) and (50), (48) yields

$$\begin{aligned} \dot{V} \leq & \sum_{i=1}^N \left[ -\sum_{m=1}^{n_i} \gamma e_{i,m}^2 + \sum_{m=1}^{n_i} (\tilde{g}_{i,m} N_{i,m}(\kappa_{i,m}) + 1) \dot{\kappa}_{i,m} - \frac{\sigma_i}{2} \tilde{\theta}_i^T \tilde{\theta}_i - \frac{1}{2} q_{i,1} \tilde{\lambda}_{i,1}^2 - \frac{1}{2} q_{i,1} \tilde{\Theta}_{i,1}^2 \right. \\ & \left. - \sum_{m=1}^{n_i} \left( \frac{1}{2} q_{i,m} \tilde{\lambda}_{i,m}^2 + \frac{1}{2} q_{i,m} \tilde{\Theta}_{i,m}^2 \right) - \frac{1}{2} l_i \tilde{Q}_i^2 - \sum_{m=1}^{n_i-1} \frac{1}{\tau_{i,m+1}^*} \varpi_{i,m+1}^2 \right] + D \end{aligned}$$

Fig. 19. Adaptive parameter  $\kappa_{i,j}$  in Example B.

$$\leq -\beta V + \sum_{i=1}^N \left[ \sum_{m=1}^{n_i} (\check{g}_{i,m} N_{i,m}(\kappa_{i,m}) - 1) \dot{\kappa}_{i,m} \right] + D, \quad (51)$$

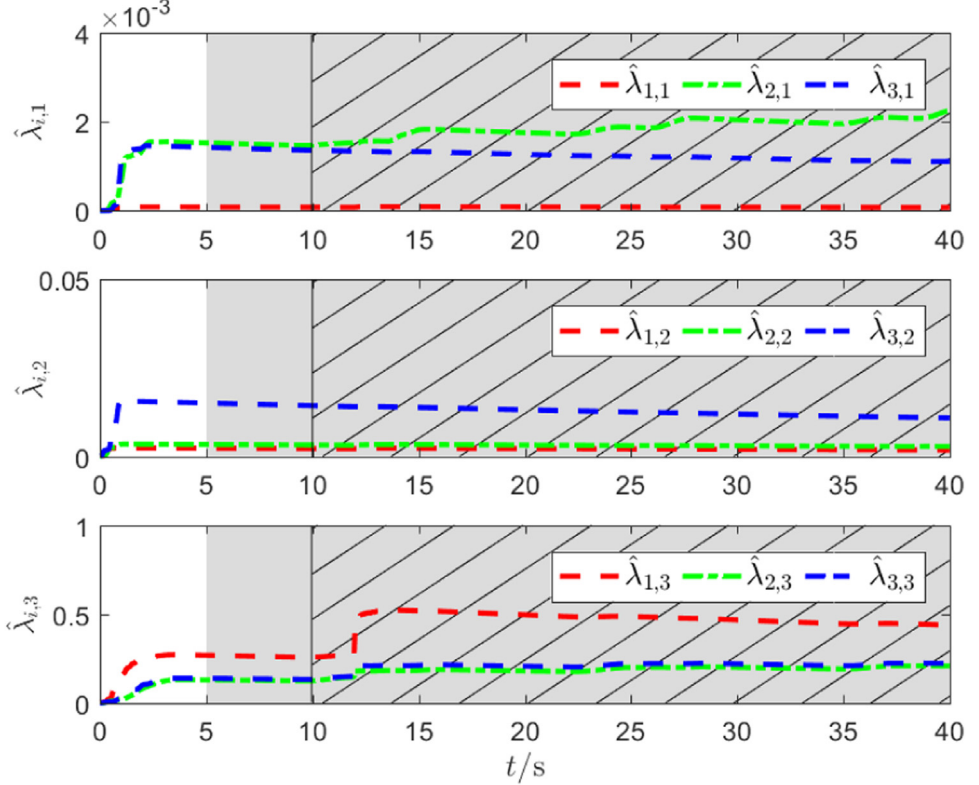
where  $\beta = \min\{1\gamma, \frac{2}{\tau_{i,m+1}^*}, \sigma_i, q_{i,1}, \dots, q_{i,n_i}, \underline{q}_{i,1}, \dots, \underline{q}_{i,n_i}, l_i\}$ .

Multiplying both sides of inequality (51) by  $\exp(\beta t)$ , and integrating on both sides of  $[0, \infty)$ , one has

$$\begin{aligned} \int_0^t \exp(\beta \tau) \dot{V}(\tau) d\tau &\leq - \int_0^t \beta \exp(\beta \tau) V(\tau) d\tau \\ &+ \sum_{i=1}^N \left[ \sum_{m=1}^{n_i} \int_0^t (\check{g}_{i,m} N_{i,m}(\kappa_{i,m}) + 1) \dot{\kappa}_{i,m} \exp(\beta \tau) d\tau \right] \\ &+ \int_0^t D \exp(\beta \tau) d\tau. \end{aligned} \quad (52)$$

This gives

$$V(t) \leq \frac{D}{\beta} + V(0) + \exp(-\beta t) \sum_{i=1}^N \left[ \sum_{m=1}^{n_i} \int_0^t (\check{g}_{i,m} N_{i,m}(\kappa_{i,m}) + 1) \dot{\kappa}_{i,m} \exp(\beta \tau) d\tau \right]. \quad (53)$$

Fig. 20. Adaptive parameter  $\hat{\lambda}_{i,j}$  in Example B.

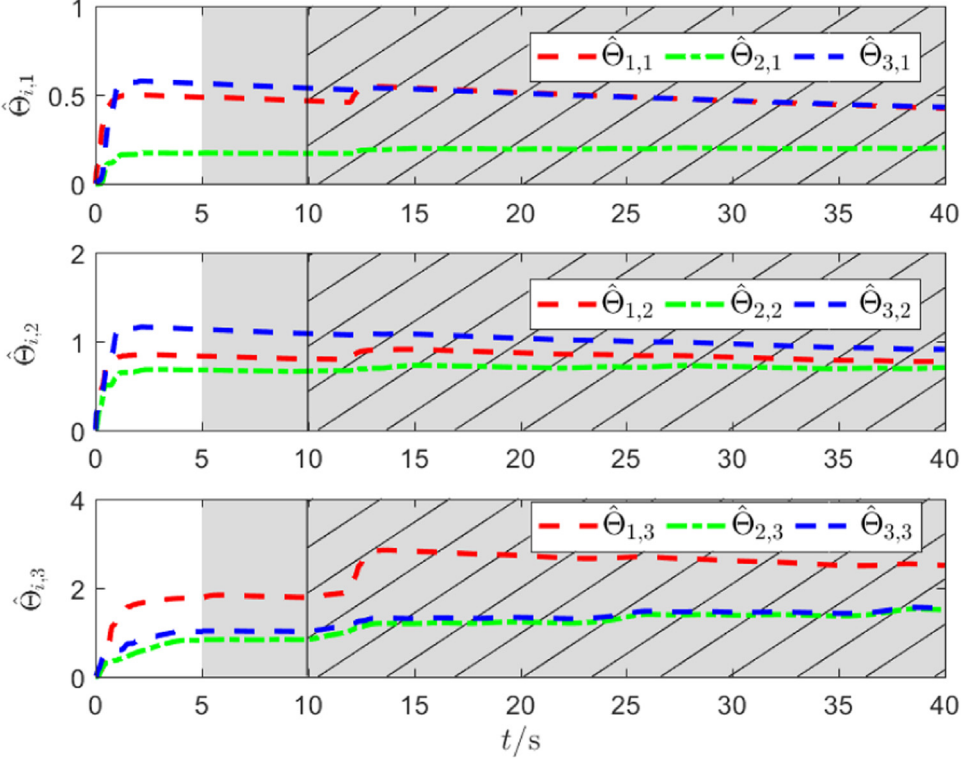
According to [Lemma 1](#), we obtain that  $\kappa_{i,m}$ ,  $V$  and  $\exp(-\beta t) \sum_{i=1}^N [\sum_{m=1}^{n_i} \int_0^t (\check{g}_{i,m} N_{i,m}(\kappa_{i,m}) + 1) \dot{\kappa}_{i,m} \exp(\beta t) d\tau] \leq \Delta$  are bounded. Thus,  $e_{i,m}^2$  are bounded over  $[0, \infty)$ , i.e.,  $\lim_{t \rightarrow \infty} e_{i,1} \leq \sqrt{2\bar{D}}$ , where  $\bar{D} = D/\beta + V(0) + \Delta$ .

Denote  $e_1 = [e_{1,1}, \dots, e_{N,1}]^T$ ,  $\check{S}_i = \check{y}_i - y_r$ , and  $\check{S} = [\check{S}_1, \dots, \check{S}_N]^T$ . From the graph theory and [Eq. \(9\)](#), we get

$$e_1 = ((\mathcal{L} + \mathcal{B}) \otimes I_N) \check{S}. \quad (54)$$

According to [Lemma 1](#) and  $\lim_{t \rightarrow \infty} e_{i,1} \leq \sqrt{2\bar{D}}$ , the result  $\lim_{t \rightarrow \infty} \|e_1\| \leq N\sqrt{2\bar{D}}$  comes. Due to the fact that the directed graph  $\mathcal{G}_0$  contains a spanning tree, we get  $\text{rank}(\mathcal{L}_0) = N$ . Then, from  $(\mathcal{L} + \mathcal{B})1_N = b$ ,  $\mathcal{L} + \mathcal{B}$  and  $b$  are linear correlation, i.e.,  $\text{rank}(\mathcal{L} + \mathcal{B}) = N$  holds, where  $1_N$  is a  $N \times 1$  column vector and all elements are 1. Thus,  $\mathcal{L} + \mathcal{B}$  is nonsingular. Accordingly,  $\lim_{t \rightarrow \infty} \|S\| = \lim_{t \rightarrow \infty} \|\check{S}\| + \|\delta_{s,i}\| \leq \|((\mathcal{L} + \mathcal{B}) \otimes I_N)^{-1} N\sqrt{2\bar{D}} + \|\delta_{s,i}\| = \sigma$ , where  $\delta_{s,i} = [\delta_{s,1,1}, \dots, \delta_{s,N,1}]^T$ , and then, the outputs from  $N$  followers can be consensus with the leader's trajectory  $y_r$ .  $\square$

**Remark 8.** From bounded initial conditions, we construct a compact set  $\Omega_1 := \{\check{x}_{1,2}^2(0) + \check{x}_{2,2}^2(0) + \dots + \check{x}_{N,2}^2(0) \leq D_1\}$  related to input signals of the function  $\bar{f}_i$ , where  $D_1$  is a positive constant. From stability analysis, the elements in  $\Omega_1$  also remain bounded by our control

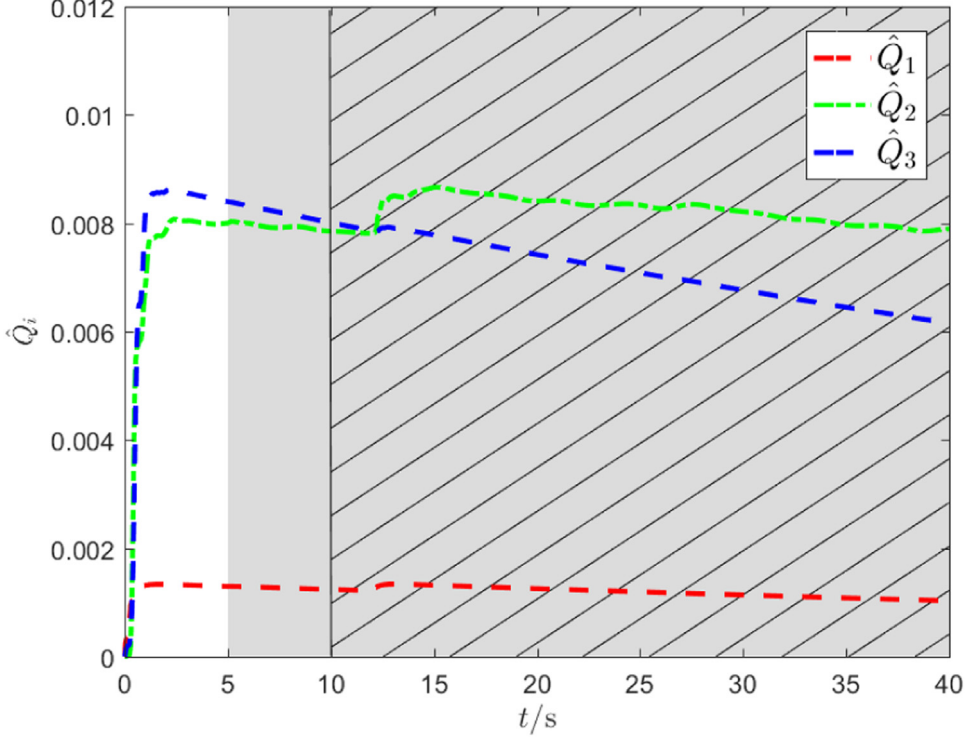
Fig. 21. Adaptive parameter  $\hat{\Theta}_{1,j}$  in Example B.

strategy. Then, we have a compact set  $\Omega_2 := \{\ddot{x}_{1,2}^2(t) + \ddot{x}_{2,2}^2(t) + \dots + \ddot{x}_{N,2}^2(t) \leq D_2\}$ , where  $D_2$  is a positive constant. The two compacts  $\Omega_1$  and  $\Omega_2$  provide a feasible compact set  $\Omega$  for NNs approximation, where  $\Omega_1 \subseteq \Omega$  and  $\Omega_2 \subseteq \Omega$ . More details can be found in [40,41].

**Remark 9.** The result  $\lim_{t \rightarrow \infty} \|S\| \leq \|(\mathcal{L} + \mathcal{B}) \otimes I_N\|^{-1} \|N\sqrt{2\bar{D}} + \|\delta_{s,i}\| = \sigma$  reveals that we can reduce the size of  $\bar{D}$  by adjusting the parameters to make the consensus error  $S_i$  small in a fixed communication topology. From the result of  $\bar{D} = D/\beta + V(0) + \Delta$ , the value of  $\bar{D}$  is related to  $\beta$  and  $D$  directly. If we scale the gains  $\Gamma_i$  and  $k_{i,m}$  up, the size of the compact  $\beta$  tends to be larger, and the value of  $\bar{D}$  decreases correspondingly. Also, if we reduce values of the gains  $p_{i,1}$ ,  $\underline{p}_{i,1}$ ,  $q_{i,m}$ ,  $\underline{q}_{i,m}$  and  $\tau_{i,m}$ , the size of the compact  $D$  tends to be small. Actually, the control input is related to these gains, and overlarge control input is not feasible. We thus have to make compromise between increasing  $\beta$  and decreasing  $D$ . Due to the fact that  $\sigma$  includes the bounded attack signals  $\|\delta_{s,i}\|$ , we are only able to alleviate the impact from attacks on the consensus performance as much as possible, and not able to remove them completely.

## 5. Simulation results

In this section, a numerical example and a group of electromechanical systems are given to verify the effectiveness of the proposed secure consensus strategy.

Fig. 22. Adaptive parameter  $\hat{Q}_i$  in Example B.

**Example 1.** A nonlinear MAS consists of four strict-feedback followers

$$\begin{cases} \dot{x}_{i,1} = f_{i,1}(\bar{x}_{i,1}) + g_{i,1}x_{i,2}, \\ \dot{x}_{i,2} = f_{i,2}(\bar{x}_{i,2}) + g_{i,2}u_i, \end{cases} \quad (55)$$

where  $f_{1,1} = \cos(x_{1,1})$ ,  $f_{1,2} = x_{1,1}x_{1,2}$ ,  $g_{1,1} = 1 + x_{1,1}^2$ ,  $g_{1,2} = 3 + \cos(x_{1,1}x_{1,2})$ ,  $f_{2,1} = \cos(0.5x_{2,1})$ ,  $f_{2,2} = x_{2,1}x_{2,2} \exp(-0.3x_{2,2})$ ,  $g_{2,1} = 1 + x_{2,1}^2$ ,  $g_{2,2} = 3 + \cos(x_{2,1}x_{2,2})$ ,  $f_{3,1} = x_{3,1} \exp(-0.5x_{3,1})$ ,  $f_{3,2} = x_{3,1}x_{3,2}^2$ ,  $g_{3,1} = 1 + x_{3,1}^2$ ,  $g_{3,2} = 3 + \cos(x_{3,1}x_{3,2})$ ,  $f_{4,1} = \sin(-0.7x_{4,1})$ ,  $f_{4,2} = 0.3x_{4,1}x_{4,2}^2$ ,  $g_{4,1} = 1 + x_{4,1}^2$ , and  $g_{4,2} = 3 + \cos(x_{4,1}x_{4,2})$ . A directed topology is shown in Fig. 4. The dead-zone parameter are  $p_{ir} = 0.1$ ,  $p_{il} = 0.1$ ,  $H_{il} = (1 - 0.2 \sin(v_i))$ ,  $H_{ir} = (0.8 - 0.1 \cos(v_i))$ . The trajectory of the leader is  $y_r = 0.5(\sin(t) + \sin(0.5t))$ . Sensor attacks  $\delta_{s,i} = 0.5(0.1 \sin(t) - 0.8)$  and actuator attacks  $\Delta a_i = 0.5$  inflict during 5s-50s and 10s-50s, respectively. The control parameters are  $k_{i,1} = 12$ ,  $k_{i,2} = 10$ ,  $q_{i,m} = 0.5$ ,  $\underline{q}_{i,m} = 0.02$ ,  $p_{i,1} = \underline{p}_{i,1} = 0.05$ ,  $\tau_{i,2} = 0.05$ ,  $\Gamma_i = 2$ ,  $\gamma_i = 0.02$  and  $l_i = 0.05$ ,  $i = 1, \dots, 4$ ,  $m = 1, 2$ . The initial states are set as  $[x_{1,1}(0), x_{1,2}(0), x_{2,1}(0), x_{2,2}(0), x_{3,1}(0), x_{3,2}(0), x_{4,1}(0), x_{4,2}(0)]^T = [0.15, 0.2, 0.1, 0.3, -0.1, 0.2, -0.2, 0.1]^T$ . Fig. 5 shows the trajectories of the leader and four followers steered by our distributed secure consensus control strategy. Fig. 6 is the dead-zone input of four followers. Figs. 7–13 are the curves of Nussbaum functions and adaptive parameters. It can be seen that when the MAS under sensor and actuator attacks

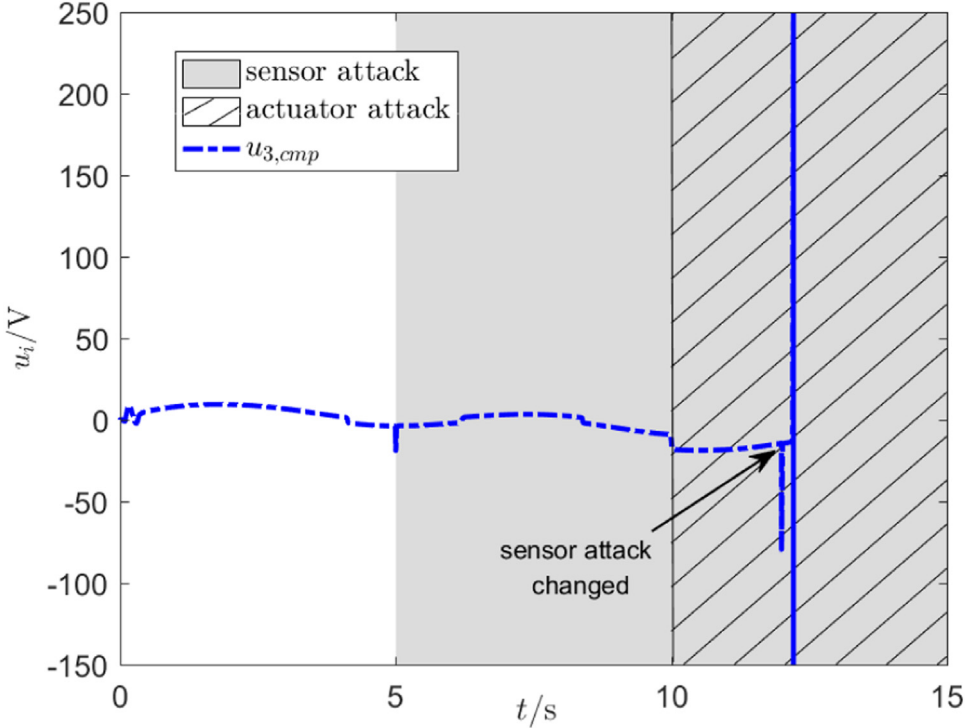


Fig. 23. Control input of the 3rd follower without sensor attack treatment [23] in Example B.

begin at 5s and 10s, respectively, our secure control strategy quickly responds and ensures that the output of each follower achieve consensus with the trajectory of the leader.

Although many same techniques, such as backstepping, Nussbaum function and continuous function separation theorem, are used in our paper and the method in [33]: (1) The followers' uncertain term in [33] is a linear parametrization condition, and the control direction is an unknown constant. In our paper, uncertainties and the control direction are unknown functions. (2) In [33], control directions in  $m$ -th subsystem of each follower are 1,  $m = 1, \dots, n-1$ . It is not necessary to introduce Nussbaum functions in each virtual control law. In our paper, control directions are unknown in each subsystem of followers. For this end, we introduce Nussbaum functions into each virtual control law in our strategy. (3) A leaderless consensus control for an MAS is studied with neighbor information suffered from sensor attacks in [33], and there is not any treatment for the paralyzed neighbor information. In our leader-follower consensus control, the continuous function separation theorem is employed to separate attack-related signals in neighbor information, and an adaptive parameter is designed to compensate them. (4) A normal actuator is paralyzed in [33], and the control method in [33] has no capability of dealing with a dead zone. In our strategy, to against the dead-zone actuator under attacks, we employ the continuous function separation theorem and design adaptive parameters.

In order to illustrate the secure performance of our control strategy, we compare simulation results by our strategy with that by the traditional consensus method [42]. The same initial

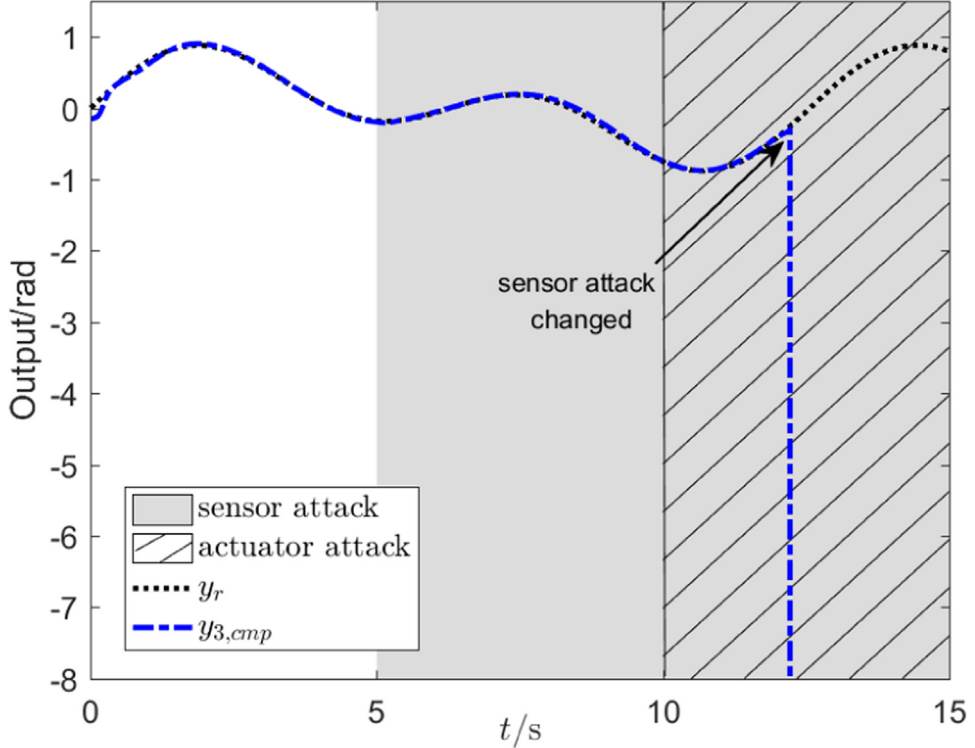


Fig. 24. Angular positions of the leader and the 3rd follower without sensor attack treatment [23] in Example B.

conditions and attacks are set. Fig. 14 shows the comparison results, where the notation ‘cmp’ in the subscripts are denoted as the traditional consensus method [42]. It can be seen from Fig. 14 that the outputs of the 2nd and 4th follower appear divergence as the actuator attacks are added at 10s, and this reveals that the traditional consensus method, without secure technique, is not able to cope with this attack effectively.

**Example 2.** We consider a group of electro-mechanical systems [4], and the dynamics of individual follower are

$$\begin{cases} \dot{x}_{i,1} = x_{i,2}, \\ \dot{x}_{i,2} = \frac{1}{M_i}x_{i,3} - \frac{\bar{N}_i}{M_i} \sin x_{i,1} - \frac{\bar{B}_i}{M_i}x_{i,2}, \\ \dot{x}_{i,3} = \frac{u_i}{L_i} - \frac{\bar{K}_i}{L_i}x_{i,2} - \frac{\bar{R}_i}{L_i}x_{i,3}, \\ y_i = x_{i,1}, \end{cases} \quad (56)$$

where  $x_{i,1} = q_i$  is the  $i$ th motor angular position,  $x_{i,2} = \dot{q}_i$ ,  $x_{i,3} = I_i$  is the armature current,  $u_i$  is the input voltage,  $\bar{M}_i = \frac{\bar{J}_i}{\bar{K}_{it}} + \frac{\bar{m}_i\bar{L}_{i0}^2}{3\bar{K}_{it}} + \frac{\bar{M}_{i0}\bar{L}_{i0}^2}{\bar{K}_{it}} + \frac{2\bar{M}_{i0}\bar{R}_{i0}^2}{5\bar{K}_{it}}$ ,  $\bar{N}_i = \frac{\bar{m}_i\bar{L}_{i0}G}{2\bar{K}_{it}} + \frac{\bar{M}_{i0}\bar{L}_{i0}G}{\bar{K}_{it}}$ ,  $\bar{B}_i = \frac{\bar{B}_{i0}}{\bar{K}_{it}}$ ,  $\bar{J}_i = 1.625 \times 10^{-3} \text{ kg} \cdot \text{m}^2$ ,  $\bar{m}_i = 0.506 \text{ kg}$ ,  $\bar{R}_{i0} = 0.023 \text{ m}$ ,  $\bar{M}_{i0} = 0.434 \text{ kg}$ ,  $\bar{L}_{i0} = 0.305 \text{ m}$ ,  $\bar{B}_{i0} = 1.625 \times 10^{-2} \text{ N} \cdot \text{m} \cdot \text{s}/\text{rad}$ ,  $\bar{L}_i = 2.5 \times 10^{-2} \text{ H}$ ,  $\bar{R}_i = 5.0 \Omega$ ,  $\bar{K}_{it} = 0.9 \text{ N} \cdot \text{m}/\text{A}$  and  $G = 9.8 \text{ N/kg}$ . Denote nonlinear system functions  $f_{i,2} = -\frac{\bar{N}_i}{M_i} \sin x_{i,1} - \frac{\bar{B}_i}{M_i}x_{i,2}$ ,  $f_{i,3} = -\frac{\bar{K}_i}{L_i}x_{i,2} - \frac{\bar{R}_i}{L_i}x_{i,3}$ , and the unknown gain are taken as  $g_{i,1} = 1$ ,  $g_{i,2} = \frac{1}{M_i}$ ,  $g_{i,3} = \frac{1}{L_i}$  and  $i = 1, 2, 3$ . The

topology of directed communication is shown in Fig. 15, and the trajectory of the leader is  $y_r = 0.5(\sin(t) + \sin(0.5t))\text{rad}$ . The sensor attack  $\delta_{s,i} = 0.5(0.3 \sin t - 0.4)$  during [5s,12s], and the actuator attack  $\Delta a_i = 5$  with the period [10s,40s]. After 12s, sensor attack are changed to  $\delta_{s,i} = 0.2(0.5 \sin(t) - 0.1)$ . The dead-zone parameter are  $p_{ri} = 1.4$ ,  $p_{li} = 1.7$ ,  $m_{li} = 1.5$ , and  $m_{ri} = 1$ . The control parameters are selected as follows  $k_{i,1} = 10$ ,  $k_{i,2} = 8$ ,  $k_{i,3} = 8$ ,  $q_{i,m} = 0.01$ ,  $q_{i,m} = 0.01$ ,  $p_{i,1} = p_{i,1} = 0.01$ ,  $\tau_{i,2} = 0.01$ ,  $\tau_{i,3} = 0.01$ ,  $\Gamma_i = 2$ , and  $\gamma_i = 0.02$ ,  $l_i = 0.05$ ,  $i = 1, \dots, 3$ ,  $m = 1, 2, 3$ . The initial states are set as  $[x_{i,1}(0), x_{i,2}(0), x_{i,3}(0)]^T = [0.1\text{rad}, 0.1\text{rad}, 0.15\text{rad}]^T$ . The simulation results are shown in Figs. 16–22. Fig. 16 shows the angular positions of the leader and four followers. It can be seen from this figure that the angular positions of all followers achieve consensus. Fig. 17 is control inputs of followers. Figs. 18–22 are curves of Nussbaum functions and adaptive parameters.

To show the advantage of our consensus secure control strategy, we also present comparison results in this example. The consensus control strategy without treatment for sensor attacks [23] is taken. Figs. 23 and 24 show the control input and output of the 3rd follower. It can be clearly seen that, without treatment for sensor attacks, the control input diverges as the intensity of malicious sensor attacks changes at 12s. Accordingly, unstable phenomenon of the output, from this electromechanical system, also appears.

## 6. Conclusion

A distributed consensus secure control strategy has been designed in this paper for a nonlinear MAS with strict-feedback followers against sensor and actuator attacks, where each follower is with unknown control directions and unknown dead-zone input. The separation theorem has been used to construct estimators to compensate for the influence of sensor and actuator attacks. Based on Lyapunov theory and graph theory knowledge, the stability analysis of closed-loop systems can be established under bounded attacks. Finally, a numerical example and a group of electromechanical systems simulation have been provided to verify the validity of the Secure strategy. Future work may direct to formation control against malicious attacks.

## Declaration of Competing Interest

The authors declare that they have no known competing financial interests or personal relationships that could have appeared to influence the work reported in this paper.

## Acknowledgments

This work was supported by Hybrid AI and Big Data Research Center of Chongqing University of Education under Grant 2023XJPT02, by the Huali Program for Excellent Talents in Nanjing University of Posts and Telecommunications, by the Natural Science Foundation of Nanjing University of Posts and Telecommunications under Grant NY220194, Grant NY221082, and Grant NY222144, and by the foundation from Key Laboratory of Industrial Internet of Things, and Networked Control of the Ministry of Education of China under Grant 2021FF01.

## References

- [1] D. Wang, Z. Wang, B. Shen, F.E. Alsaadi, T. Hayat, Recent advances on filtering and control for cyber-physical systems under security and resource constraints, J. Frankl. Inst. 353 (11) (2016) 2451–2466.

- [2] Z. Peng, J. Wang, D. Wang, Q.L. Han, An overview of recent advances in coordinated control of multiple autonomous surface vehicles, *IEEE Trans. Ind. Inf.* 17 (2) (2021) 732–745.
- [3] T. Li, W. Bai, Q. Liu, Y. Long, C.L.P. Chen, Distributed fault-tolerant containment control protocols for the discrete-time multiagent systems via reinforcement learning method, *IEEE Trans. Neural Netw. Learn. Syst.* doi:[10.1109/TNNLS.2021.3121403](https://doi.org/10.1109/TNNLS.2021.3121403).
- [4] C. Li, S. Tong, W. Wang, Fuzzy adaptive high-gain-based observer backstepping control for SISO nonlinear systems, *Inf. Sci. (Ny)* 181 (11) (2011) 2405–2421.
- [5] Q. Wang, H.E. Psilakis, C. Sun, Cooperative control of multiple agents with unknown high-frequency gain signs under unbalanced and switching topologies, *IEEE Trans. Autom. Control* 64 (6) (2019) 2495–2501.
- [6] H. Yang, T. Li, Y. Long, C.L.P. Chen, Y. Xiao, Distributed virtual inertia implementation of multiple electric springs based on model predictive control in DC microgrids, *IEEE Trans. Ind. Electron.* doi:[10.1109/TIE.2021.3130332](https://doi.org/10.1109/TIE.2021.3130332).
- [7] Z. Peng, J. Wang, D. Wang, Distributed maneuvering of autonomous surface vehicles based on neurodynamic optimization and fuzzy approximation, *IEEE Trans. Control Syst. Technol.* 26 (3) (2018) 1083–1090.
- [8] Z. Zuo, Nonsingular fixed-time consensus tracking for second-order multi-agent networks, *Automatica* 54 (2015) 305–309.
- [9] H. Hong, W. Yu, G. Wen, X. Yu, Distributed robust fixed-time consensus for nonlinear and disturbed multiagent systems, *IEEE Trans. Syst. Man Cybern. Syst.* 47 (7) (2017) 1464–1473.
- [10] X. Jin, S. Wang, J. Qin, W.X. Zheng, Y. Kang, Adaptive fault-tolerant consensus for a class of uncertain nonlinear second-order multi-agent systems with circuit implementation, *IEEE Trans. Circuits Syst. I Regul. Pap.* 65 (7) (2018) 2243–2255.
- [11] L. Zhao, G. Yang, Cooperative adaptive fault-tolerant control for multi-agent systems with deception attacks, *J. Franklin Inst.* 357 (6) (2020) 3419–3433.
- [12] D. Ye, S. Luo, A co-design methodology for cyber-physical systems under actuator fault and cyber attack, *J. Franklin Inst.* 356 (4) (2019) 1856–1879.
- [13] T. Zhang, D. Ye, False data injection attacks with complete stealthiness in cyber-physical systems: a self-generated approach, *Automatica* 120 (2020) 109117.
- [14] Y. Gao, G. Sun, J. Liu, Y. Shi, L. Wu, State estimation and self-triggered control of CPSs against joint sensor and actuator attacks, *Automatica* 113 (2020) 108687.
- [15] L. An, G.H. Yang, Improved adaptive resilient control against sensor and actuator attacks, *Inf. Sci. (Ny)* 423 (2018) 145–156.
- [16] X. Huang, J. Dong, An adaptive secure control scheme for t-s fuzzy systems against simultaneous stealthy sensor and actuator attacks, *IEEE Trans. Fuzzy Syst.* 29 (7) (2021) 1978–1991.
- [17] Y. Tan, Q. Liu, D. Du, B. Niu, S. Fei, Observer-based finite-time h control for interconnected fuzzy systems with quantization and random network attacks, *IEEE Trans. Fuzzy Syst.* 29 (3) (2021) 674–685.
- [18] G. Chen, Y. Zhang, S. Gu, W. Hu, Resilient state estimation and control of cyber-physical systems against false data injection attacks on both actuator and sensors, *IEEE Trans. Control Netw. Syst.* 9 (1) (2022) 500–510.
- [19] K. Bansal, P. Mukhija, Aperiodic sampled-data control of distributed networked control systems under stochastic cyber-attacks, *IEEE/CAA J. Autom. Sin.* 7 (4) (2020) 1064–1073.
- [20] H. Modares, B. Kiumarsi, F.L. Lewis, F. Ferrese, A. Davoudi, Resilient and robust synchronization of multiagent systems under attacks on sensors and actuators, *IEEE Trans. Cybern* 50 (3) (2020) 1240–1250.
- [21] C. Hua, L. Zhang, X. Guan, Distributed adaptive neural network output tracking of leader-following high-order stochastic nonlinear multiagent systems with unknown dead-zone input, *IEEE Trans. Cybern* 47 (1) (2017) 177–185.
- [22] H. Su, W. Zhang, Adaptive fuzzy control of stochastic nonlinear systems with fuzzy dead-zones and unmodeled dynamics, *IEEE Trans. Cybern* 50 (2) (2020) 587–599.
- [23] K. Lu, Z. Liu, G. Lai, Y. Zhang, C.L.P. Chen, Adaptive fuzzy tracking control of uncertain nonlinear systems subject to actuator dead-zone with piecewise time-varying parameters, *IEEE Trans. Fuzzy Syst.* 27 (7) (2019) 1493–1505.
- [24] Y.-H. Jing, G.H. Yang, Fuzzy adaptive fault-tolerant control for uncertain nonlinear systems with unknown dead-zone and unmodeled dynamics, *IEEE Trans. Fuzzy Syst.* 27 (12) (2019) 2265–2278.
- [25] Y.-J. Liu, S. Li, S. Tong, C.L.P. Chen, Adaptive reinforcement learning control based on neural approximation for nonlinear discrete-time systems with unknown nonaffine dead-zone input, *IEEE Trans. Neural Netw. Learn. Syst.* 30 (1) (2019) 295–305.

- [26] F. Shojaei, M.M. Arefi, A. Khayatian, H.R. Karimi, Observer-based fuzzy adaptive dynamic surface control of uncertain nonstrict feedback systems with unknown control direction and unknown dead-zone, *IEEE Trans. Syst. Man Cybern. Syst.* 49 (1) (2019) 2340–2351.
- [27] R.D. Nussbaum, Some remarks on a conjecture in parameter adaptive control, *Syst. Control Lett.* 3 (5) (1983) 243–246.
- [28] Q. Wang, H.E. Psillakis, C. Sun, F.L. Lewis, Adaptive NN distributed control for time-varying networks of nonlinear agents with antagonistic interactions, *IEEE Trans. Neural Netw. Learn Syst.* 32 (6) (2021) 2573–2583.
- [29] Q. Wang, C. Sun, Adaptive consensus of multiagent systems with unknown high-frequency gain signs under directed graphs, *IEEE Trans. Syst. Man Cybern. Syst.* 50 (6) (2020) 2181–2186.
- [30] S. Yin, H. Gao, J. Qiu, O. Kaynak, Adaptive fault-tolerant control for nonlinear system with unknown control directions based on fuzzy approximation, *IEEE Trans. Syst. Man Cybern. Syst.* 47 (8) (2017) 1909–1918.
- [31] Z. Yu, S. Li, Z. Yu, F. Li, Adaptive neural output feedback control for nonstrict-feedback stochastic nonlinear systems with unknown backlash-like hysteresis and unknown control directions, *IEEE Trans. Neural Netw. Learn Syst.* 29 (4) (2018) 1147–1160.
- [32] H. Rezaee, F. Abdollahi, Adaptive consensus control of nonlinear multiagent systems with unknown control directions under stochastic topologies, *IEEE Trans. Neural Netw. Learn. Syst.* 29 (8) (2018) 3538–3547.
- [33] R. Gao, J. Huang, L. Wang, Leaderless consensus control of uncertain multi-agents systems with sensor and actuator attacks, *Inf. Sci. (Ny)* 505 (2019) 144–156.
- [34] Y.-J. Liu, Y. Gao, S. Tong, Y. Li, Fuzzy approximation-based adaptive backstepping optimal control for a class of nonlinear discrete-time systems with dead-zone, *IEEE Trans. Fuzzy Syst.* 24 (1) (2016) 16–28.
- [35] E.W. Bai, *Adaptive Dead Zone Inverse for Possibly Nonlinear control Systems*, Springer, 2001. Berlin, Germany
- [36] B. Genge, I. Kiss, P. Haller, A system dynamics approach for assessing the impact of cyber attacks on critical infrastructures, *Int. J. Crit. Infrastruct. Prot.* 10 (2015) 3–17.
- [37] S. Parkinson, P. Ward, K. Wilson, J. Miller, Cyber threats facing autonomous and connected vehicles: future challenges, *IEEE Trans. Intell. Transp. Syst.* 18 (11) (2017) 2898–2915.
- [38] Y. Guan, X. Ge, Distributed attack detection and secure estimation of networked cyber-physical systems against false data injection attacks and jamming attacks, *IEEE Trans. Signal Inf. Process. Netw.* 4 (1) (2018) 48–59.
- [39] D. Swaroop, J.K. Hedrick, P.P. Yip, J.C. Gerdes, Dynamic surface control for a class of nonlinear systems, *IEEE Trans. Autom. Control* 45 (10) (2000) 1893–1899.
- [40] D. Wang, J. Huang, Neural network-based adaptive dynamic surface control for a class of uncertain nonlinear systems in strict-feedback form, *IEEE Trans. Neural Netw.* 16 (1) (2005) 195–202.
- [41] S.S. Ge, C. Wang, Adaptive neural control of uncertain MIMO nonlinear systems, *IEEE Trans. Neural Netw.* 15 (3) (2004) 674–692.
- [42] T. Li, D. Wang, G. Feng, S. Tong, A DSC approach to robust adaptive NN tracking control for strict-feedback nonlinear systems, *IEEE Trans. Syst. Man Cybern. Part B (Cybern.)* 40 (3) (2010) 915–927.
- [43] X. Shao, D. Ye, Fuzzy adaptive event-triggered secure control for stochastic nonlinear high-order MASs subject to dos attacks and actuator faults, *IEEE Trans. Fuzzy Syst.* 29 (12) (2021) 3812–3821.
- [44] W. Liu, C. Qian, Adaptive control of nonlinearly parameterized systems: the smooth feedback case, *IEEE Trans. Autom. Control* 47 (8) (2002) 1249–1266.